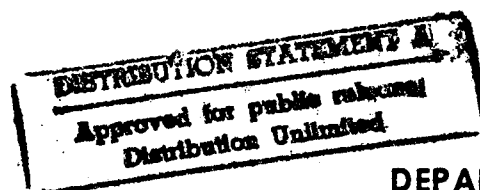


19941228 025



DEPARTMENT OF THE AIR FORCE  
AIR UNIVERSITY  
**AIR FORCE INSTITUTE OF TECHNOLOGY**

Wright-Patterson Air Force Base, Ohio

AFIT/GAP/ENP/94D-8

FEASIBILITY EXPLORATION OF THROUGHFOLD  
AS A PREDICTOR FOR TARGET LOADING  
AND ASSOCIATED ERROR BOUNDS

THESIS

Kris G. Rongone, B.S.  
Captain, USAF

AFIT/GAP/ENP/94D-8

DTIC QUALITY INSPECTED 2

Approved for public release; distribution unlimited

# REPORT DOCUMENTATION PAGE

Form Approved  
OMB No. 0704-0188

Public reporting burden for this collection of information is estimated to average 1 hour per response, including the time for reviewing instructions, searching existing data sources, gathering and maintaining the data needed, and completing and reviewing the collection of information. Send comments regarding this burden estimate or any other aspect of this collection of information, including suggestions for reducing this burden, to Washington Headquarters Services, Directorate for Information Operations and Reports, 1215 Jefferson Davis Highway, Suite 1204, Arlington, VA 22202-4302, and to the Office of Management and Budget, Paperwork Reduction Project (0704-0188), Washington, DC 20503.

1. AGENCY USE ONLY (Leave blank)		2. REPORT DATE Dec 1994		3. REPORT TYPE AND DATES COVERED Master's Thesis	
4. TITLE AND SUBTITLE FEASIBILITY EXPLORATION OF THROUGHFOLD AS A PREDICTOR FOR TARGET LOADING AND ASSOCIATED ERROR BOUNDS				5. FUNDING NUMBERS	
6. AUTHOR(S) Kris G. Rongone, Captain, USAF					
7. PERFORMING ORGANIZATION NAME(S) AND ADDRESS(ES) Air Force Institute of Technology 2750 P Street WPAFB OH 45433-6583				8. PERFORMING ORGANIZATION REPORT NUMBER AFIT/GAP/ENP/94D-8	
9. SPONSORING / MONITORING AGENCY NAME(S) AND ADDRESS(ES) N/A				10. SPONSORING / MONITORING AGENCY REPORT NUMBER	
11. SUPPLEMENTARY NOTES					
12a. DISTRIBUTION / AVAILABILITY STATEMENT APPROVED FOR PUBLIC RELEASE; DISTRIBUTION UNLIMITED.				12b. DISTRIBUTION CODE	
13. ABSTRACT (Maximum 200 words)  <p>Various applications of the Fredholm integral equation appear in different fields of study. An application of particular interest to the Air Force arises in determination of target loading from nuclear effects simulations. Current techniques first unfold the incident spectrum then determine target loading; resulting spectrum and loading are assumed exact.</p> <p>This study investigates the feasibility of a new method, through-fold, for directly determining defensible error bounds on target loading. Through-fold uses <i>a priori</i> information to define input data and represents target response with a linear combination of instrument responses plus a remainder to derive a quadratic expression for exact target loading. This study uses a simplified, linear version of the quadratic expression.</p> <p>Through-fold feasibility is tested by comparing error bounds based on three target loading functions. The three test cases include an exact linear combination of instrument responses, the same combination plus a positive remainder, and the same combination plus a negative remainder.</p> <p>Total error bounds reduced from 100% to 35% in cases #1 and #2. In case #3 error bound was reduced to 48%. These results indicate that through-fold has promise as a predictor of error bounds on target loading.</p>					
14. SUBJECT TERMS NUCLEAR INSTRUMENTATION, SPECTRAL ENERGY DISTRIBUTION, RADIATION SIMULATION TESTS, OPTIMIZATION, THROUGH-FOLD, RADIATION INSTRUMENTS				15. NUMBER OF PAGES 110	
				16. PRICE CODE	
17. SECURITY CLASSIFICATION OF REPORT Unclassified	18. SECURITY CLASSIFICATION OF THIS PAGE Unclassified	19. SECURITY CLASSIFICATION OF ABSTRACT Unclassified	20. LIMITATION OF ABSTRACT UL		

FEASIBILITY EXPLORATION OF THROUGHFOLD AS A PREDICTOR  
FOR TARGET LOADING AND ASSOCIATED ERROR BOUNDS

THESIS

Presented to the Faculty of the Graduate School of Engineering

of the Air Force Institute of Technology

Air Education and Training Command

In Partial Fulfillment of the

Requirements for the Degree of

Master of Science in Nuclear Engineering

Kris G. Rongone, B.S.

Captain, USAF

December 1994

<b>Accession For</b>	
NTIS GRA&I	<input checked="checked" type="checkbox"/>
DTIC TAB	<input type="checkbox"/>
Unannounced	<input type="checkbox"/>
Justification	
By	
Distribution/	
Availability Codes	
Dist	Avail and/or Special
A-1	

Approved for public release; distribution unlimited

## Preface

The purpose of this study was to explore the capability of a new method, through-fold, as a predictor of defensible error bounds on target loading. There were two specific goals. First, to develop the required derivation of a bounded definition for target loading. Second, to develop a method for implementing through-fold for verification of expected performance.

Users of current unfolding processes have a need for theoretically based error estimates of target loading in the evaluation of nuclear effects simulations. However, due to an inherent ill-posedness, current methods lack the capability for determining error bounds.

Guidance and support during this study was received from many individuals. First, I am indebted to my faculty advisor, Professor Kirk A. Mathews, for his help and extreme patience during this study. His expertise in the field and knowledge of *Mathematica* proved invaluable. Next I would like to thank Capt. Russell Daniel and Capt. Dennis Miller. Their work on unfolding problems was crucial to my understanding of the topic. Finally I would like to thank my roommates Ron, Mike, and Michelle for their help and for just putting up with me during the thesis quarters.

Kris G. Rongone

## Table of Contents

	Page
Preface .....	ii
List of Figures .....	v
List of Tables .....	vi
List of Notation .....	vii
Abstract .....	viii
I. Introduction .....	1
Background .....	1
Problem .....	3
Scope .....	3
Assumption .....	4
General Approach .....	5
Sequence of Presentation .....	6
II. Theoretical Development .....	7
Introduction .....	7
Detection System .....	7
Sources of Error .....	14
Preliminary Derivation .....	15
Differences in the Full Derivation .....	28
Through-fold Expectations .....	30
III. Computer Implementation .....	33
Introduction .....	33
Platform .....	33
Input Data .....	33
Error Considerations .....	37
Optimization Routines .....	38
ThruFold.ma .....	39

IV.	Validation and Testing .....	40
	Introduction .....	40
	Validation .....	40
	Testing .....	45
V.	Summary and Conclusions .....	61
	Summary .....	61
	Conclusions .....	62
VI.	Recommendations .....	63
	Appendix A: Formal Derivation of Through-fold Equations .....	64
	Appendix B: Final <i>Mathematica</i> Code .....	78
	Appendix C: Additional Test Results .....	91
	Bibliography .....	99
	Vita .....	100

## List of Figures

Figure		Page
Figure 1.	Typical Open Response Function .....	9
Figure 2.	Typical Closed Response Function .....	11
Figure 3.	Closed Response Functions, Instruments 1-11 .....	12
Figure 4.	Open Response Functions, Instruments 12-17 .....	13
Figure 5.	Validation Planckian Spectrum .....	34
Figure 6.	Validation Target Response Function .....	35
Figure 7.	Test Target Response Function, Variation A .....	47
Figure 8.	Test Target Response Function, Variation B .....	48
Figure 9.	Test Target Response Function, Variation C .....	48
Figure 10.	Test Target Response Function, Variation D .....	49
Figure 11.	Defined Test $T_{\bar{a}}(E)$ , Variation A .....	49
Figure 12.	Defined Test $T_{\bar{a}}(E)$ , Variation B .....	50
Figure 13.	Defined Test $T_{\bar{a}}(E)$ , Variation C .....	50
Figure 14.	Defined Test $T_{\bar{a}}(E)$ , Variation D .....	51
Figure 15.	Optimized Remainder (Upper Bound), $T_{\bar{a}}(E)$ , for T1.D .....	55
Figure 16.	Case T1.C, Defined and Optimized (Upper Bound) $T_{\bar{a}}(E)$ .....	56
Figure 17.	Case T2.D, Defined and Optimized (Upper Bound) $T_{\bar{a}}(E)$ .....	58
Figure 18.	Case T3.C, Defined and Optimized (Upper Bound) $T_{\bar{a}}(E)$ .....	59



## List of Tables

Table		Page
Table 1.	Detector K-Edge Ratios .....	12
Table 2.	Relative Error Due to Numeric Approximation of Integral .....	15
Table 3.	Validation Results (Bounds on Target Loading), Closed Instruments .....	41
Table 4.	Validation Results, (Bounds on Target Loading), Open Instruments .....	44
Table 5.	Test Results for Case T1.A .....	52
Table 6.	Test Results for Case T1.D .....	54
Table 7.	Test Results for Case T2.D .....	57
Table 8.	Test Results for Case T3.D .....	60
Table 9.	Test Results for Case T1.B .....	91
Table 10.	Test Results for Case T1.C .....	92
Table 11.	Test Results for Case T2.A .....	93
Table 12.	Test Results for Case T2.B .....	94
Table 13.	Test Results for Case T2.C .....	95
Table 14.	Test Results for Case T3.A .....	96
Table 15.	Test Results for Case T3.B .....	97
Table 16.	Test Results for Case T3.C .....	98

## List of Notation

<u>Symbol</u>	<u>Definition</u>
$a_i$	linear coefficients for target loading
$dR$	fractional instrument calibration error
$dR^+$	magnitude of upper $dR$ bound
$dR^-$	magnitude of lower $dR$ bound
$dS$	fractional spectrum error
$dS^+$	magnitude of upper $dS$ bound
$dS^-$	magnitude of lower $dS$ bound
$dT$	fractional target loading error
$dT^+$	magnitude of upper $dT$ bound
$dT^-$	magnitude of lower $dT$ bound
$dY$	fractional measurement error
$dY^+$	magnitude of upper $dY$ bound
$dY^-$	magnitude of lower $dY$ bound
$E$	energy
$N$	number of energy groups (bins)
$R$	instrument response
$S$	radiation spectrum
$T$	target response
$T_a(E)$	linear correction for target loading
$Y$	instrument signal
$Z$	target loading
$E_i^0$	fluorescer k-edge of $i^{\text{th}}$ detector
$E_i^1$	filter k-edge of $i^{\text{th}}$ detector
$\delta R$	instrument response correction
$\delta S$	spectrum correction
$\delta T$	target response correction
$\delta Y$	instrument signal correction
$\Delta E$	width of energy bin
$\sim$	tilde, denotes an exact quantity

Abstract

Various applications of the Fredholm integral equation appear in different fields of study. An application of particular interest to the Air Force arises in determination of target loading from nuclear effects simulations. Current techniques first unfold the incident spectrum then determine target loading; resulting spectrum and loading are assumed exact.

This study investigates the feasibility of a new method, through-fold, for directly determining defensible error bounds on target loading. Through-fold uses *a priori* information to define input data and represents target response with a linear combination of instrument responses plus a remainder to derive a quadratic expression for exact target loading. This study uses a simplified, linear version of the quadratic expression.

Through-fold feasibility is tested by comparing error bounds based on three target loading functions. The three test cases include an exact linear combination of instrument responses, the same combination plus a positive remainder, and the same combination plus a negative remainder.

Total error bounds reduced from 100% to 35% in cases #1 and #2. In the third test case error bound was reduced to 48%. These results indicate that through-fold has promise as a predictor of error bounds on target loading.

# FEASIBILITY EXPLORATION OF THROUGH-FOLD AS A PREDICTOR FOR TARGET LOADING AND ASSOCIATED ERROR BOUNDS

## I. Introduction

### Background

Fredholm integral equations of the first kind apply in many fields of study including acoustics, optics, geophysics, and aerodynamics (Daniel, 1988:Ch1, 1). Of particular interest to the Air Force is the measurement of pulsed radiation emitted from nuclear weapons tests. These measurements can be used to predict nuclear weapons effects on hardware by folding the incident spectrum with the hardware response function. However, the Fredholm integral equations are first used to determine the radiation spectrum incident on the equipment. The terminology in this study originates from this application.

The Fredholm integral equation of the first kind is:

$$Y(\epsilon) = \int_a^b S(\eta) R(\epsilon, \eta) d\eta \quad (1)$$

where

$Y(\epsilon)$  = detector output signal

$S(\eta)$  = radiation spectrum

$R(\epsilon, \eta)$  = detector response function

Currently, pulsed radiation detection is accomplished using a series of overlapping detectors covering the energy range of interest. Thus,  $\epsilon$ , is discretized as  $i$ , the detector index. However, practical aspects of data collection force several limitations on a detection system. These limitations include use of a finite number of detectors, limited detector resolution, and errors due to recording, transmitting and calibrating. The exact signal from each detector can be represented with the following simultaneous equations:

$$\tilde{Y}_i = \int_0^{\infty} \tilde{S}(E) \tilde{R}_i(E) dE \quad (2)$$

where

$\tilde{Y}_i$  = the exact signal of the  $i^{\text{th}}$  detector

$\tilde{S}(E)$  = the exact or actual spectrum emitted

$\tilde{R}_i(E)$  = the exact response of the  $i^{\text{th}}$  detector

Past efforts to resolve the incident spectra for determination of target loading (nuclear effects on hardware) have culminated in a cross-validation iterative unfold method (Miller, 1990). This method uses a predicted spectrum based on *a priori* data, the calibrated response functions of the detectors, and test data (i.e., measured detector signals) to conduct a general deconvolution of the incident spectrum. The unfolded spectrum is then smoothed to average out the fitting process discontinuities. After iterating the unfolded spectrum to an optimal point (determined using the cross-validation statistical method) the final unfolded spectrum is used as an approximation of the incident

spectrum. Typically, the analyst folds this incident spectrum with the target response function to determine target loading. Unfortunately, the unfolded incident radiation spectrum is assumed to be exactly correct because the iterative unfold method lacks an independent means of determining how well this unfolded spectrum approximates the incident spectrum.

### Problem

Since there are an infinite number of incident spectra which will produce the same detector outputs, the traditional deconvolution of the Fredholm equations is an ill-posed problem. Coupling this ill-posed problem with the assumption that the resulting unfolded spectrum is exact leads to target loading estimates lacking defensible error bounds.

The main purpose of this study is to investigate the feasibility of a new method for determination of bounds (both upper and lower) on the value for target loading. This new method (aptly termed through-fold) bypasses the intermediate step of determining the spectrum, and the inherent errors associated with this step, to directly determine defensible error bounds on target loading.

### Scope

This study develops the through-fold method to estimate target loading due to an incident spectrum. The through-fold method assumes the incident energy spectrum is predictable. Since experimental data are unavailable, this study is limited to simulated incident energy spectra. A set of synthetic test cases are developed for an energy spectrum ranging from  $1 E_1^0$  to  $64 E_1^0$ , where  $E_1^0$  is an arbitrary energy unit.

Using synthetic test cases for spectra and target responses, the exact target loading is calculated for each case via a simple folding routine. Relative errors with respect to the through-fold bounds are then compared to predict the feasibility of the through-fold technique.

### Assumptions

Along with assumptions associated with the through-fold, additional assumptions are required to be consistent with Miller's (1990) work.

1. The instrumentation system consists of 17 detectors, 6 open (fluorescer) response functions and 11 closed (filtered-fluorescer) response functions.
2. Detector resolution,  $E/\Delta E$ , is 1.5.
3. The instrument response functions,  $R_i(E)$ , are exact. The exact forms are given in Chapter II.
4. Measurement errors follow a Gaussian distribution (Carter, 1989:14-15).
5. The spectrum,  $S(E)$ , is exact subject to the estimate of uncertainty,  $\delta S(E)$ .
6. The spectrum has a non-negative flux constraint.
7. The target response function,  $T(E)$ , has a non-negative constraint.

Several other assumptions are required in the derivation and simplification of the through-fold equations; their discussions are deferred until they become relevant.

### General Approach

This study's approach is predominantly analytical. First, the exact target loading equation is developed. The equation derivation (detailed in Appendix A) bypasses the intermediate step that determines the incident spectrum, and thus some of the uncertainties associated with that process. Through-fold directly determines a bounding expression (exact correction terms are included) for the exact target loading. Upper and lower bounds for target loading are then expressed as linear programming problems which can be optimized with respect to assumed known bounds on the corrections. The elegance of the through-fold method is in the manipulation of basic definitions for exact terms to develop the final expression. An example of the definition of an exact term is:

$$\tilde{B} = B + \delta B \quad (3)$$

where

$\tilde{B}$  represents an exact value,

$B$  is a predicted or measured value

$\delta B$  is a correction term (error)

To incorporate experimental data into the equation, the exact target response function is represented by a linear combination of the instrument response functions plus a remainder. This is discussed further in Chapter II.

Second, data that would normally be available to the analyst is simulated. These data include a predicted spectrum and a conservative estimate of its error (both based on *a priori* information), the detector response functions, and a target response function. Once



the input data are developed, instrument signals are constructed by folding the simulated spectrum with the detector response functions. Measured signals are then approximated by simulating measurement error with random noise from a Gaussian distribution.

Third, the final expression is optimized over the choice of linear combinations available. This reduces the overall error spread from what would be calculated without using experimental data in the derivation.

Finally, the method is tested to confirm that the overall error spread can be reduced via through-fold.

#### Sequence of Presentation

Chapter II presents a detailed discussion of the through-fold theoretical development including potential error sources and expectations for the through-fold technique. Chapter III covers implementation of the through-fold equations to include input data, error considerations, and optimization. Chapter IV discusses the through-fold test cases and results. Chapter V presents the results of this thesis. Chapter VI presents recommendations for further study.

## II. Theoretical Development

### Introduction

Along with introducing the basic concepts of the through-fold technique, Section I defined the assumptions and goals of this study. This section provides the theoretical background of the through-fold method. The following topics are discussed: detection systems and their associated response functions, sources of error, a preliminary derivation including motivation for the approach, discussion of a more detailed derivation, and expectations of the through-fold technique.

### Detection Systems

A detector response function,  $R_i(E)$ , is the normalized output of the detector due to the portion of the incident spectrum at energy level  $E$ . The response functions are assumed to be accurately calibrated using an adjustable monoenergetic source.

In a realistic experiment, detector systems having multiple response functions are used simultaneously and their results are compared in an effort to reduce measurement error. The detectors used to measure spectra of nuclear simulations are designed to have an output proportional to an incident spectrum in the energy range  $E$  to  $E + \Delta E$  given by

$$y_i(E)\Delta E = R_i(E) S(E) \Delta E \quad (4)$$

where

$y_i(E)\Delta E$  = the incremental output of detector  $i$  due to the spectrum in the energy range  $E$  to  $E + \Delta E$

$R_i(E)$  = the response of detector  $i$  to the part of the spectrum at energy  $E$ .

$S(E) \Delta E$  = the amount of the spectrum that is in the energy range  $E$  to  $E + \Delta E$

As stated in Section I, two different types of detector systems having either open (fluorescer) or closed (filter-fluorescer) response functions are used for this study. Both detector response functions are based on simplified versions (Daniel:1988, App-A) of the detector response functions for measuring the spectra of pulsed x-radiation presented by Gorbachenko *et al.* (1976).

Open (Fluorescer) Response Functions. The open detector system uses fluorescer detectors with a zero response for photon energies less than the k-edge of the fluorescer. Photons above the k-edge of the fluorescer material react with the fluorescer, causing a cascade of x-ray fluorescence. The response decreases for energies above the fluorescer k-edge due to a decreased probability of photon reactions at the higher energies. The thickness and type of fluorescer material can be varied to achieve a desired sensitivity. The fluorescer response function used for this study is

$$R_i^{open}(E) = \begin{cases} 0 & E < E_i^0 \\ \left(\frac{1}{E}\right) \left[ 1 - \exp \left[ -3 \left( \frac{E_i^0}{E} \right)^3 \right] \right] & E \geq E_i^0 \end{cases} \quad (5)$$

where

$R_i^{open}(E)$  = the open function of the  $i^{\text{th}}$  detector

$E_i^0$  = k-edge of the fluorescer for the  $i^{\text{th}}$  detector

$E$  = energy

Figure 1 is an example of a typical open response function. In this example, the detector has a k-edge of  $2E_1^0$ , where  $E_1^0$  is defined as the lowest k-edge energy of the entire detection system. All energy units in this study are given the units of  $E_1^0$ .

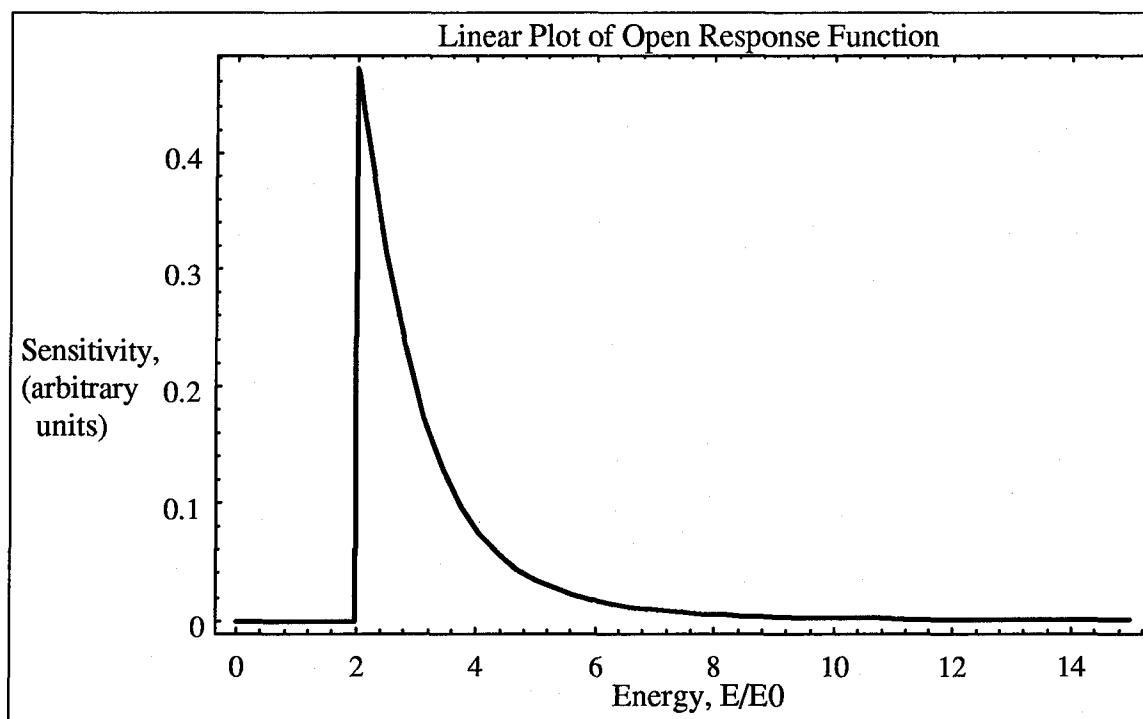


Figure 1. Typical Open Response Function

Closed (Filtered-Fluorescer) Response Functions. The closed detector system consists of a filter and a fluorescer to shape an open response between the k-edges of the filter and fluorescer (Carter, 1989:7-9). Photons above the filter k-edge interact causing fluorescence and subsequently degrade in energy. Photons getting past the filter and

having energies above the fluorescer k-edge interact at the fluorescer in a manner similar to those of the open detection system. Since the k-edges of the filter and fluorescer are different, the shape of the closed response system differs from that of an open response system (Miller, 1990:9-10). The filter-fluorescer response function used for this study is

$$R_i^{closed}(E) = \begin{cases} 0 & E \leq E_i^0 \\ \left(\frac{1}{E}\right) \left\{ 1 - \exp \left[ -2 \left( \frac{E_i^0}{E} \right)^3 \right] \right\} \exp \left[ -0.25 \left( \frac{E_i^1}{E} \right)^3 \right] & E_i^0 \leq E \leq E_i^1 \\ \left(\frac{1}{E}\right) \left\{ 1 - \exp \left[ -2 \left( \frac{E_i^0}{E} \right)^3 \right] \right\} \exp \left[ -1.5 \left( \frac{E_i^1}{E} \right)^3 \right] & E > E_i^1 \end{cases} \quad (6)$$

where

$R_i^{closed}(E)$  = the closed function of the  $i^{\text{th}}$  detector

$E_i^1$  = the k-edge of the filter for the  $i^{\text{th}}$  detector

$E_i^0$  = k-edge of the fluorescer for the  $i^{\text{th}}$  detector

$E$  = energy

Figure 2 is an example of a typical closed response function. In this example, the detector has a fluorescer k-edge of  $2E_1^0$  and a filter k-edge of  $4E_1^0$ .

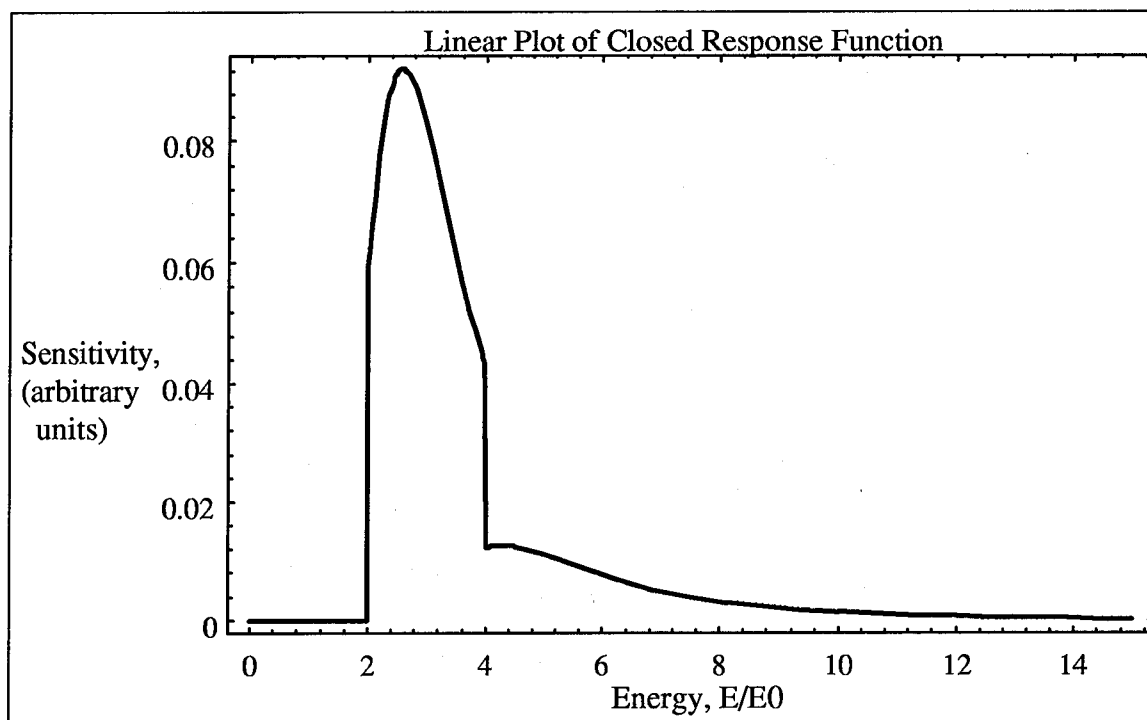


Figure 2. Typical Closed Response Function

Detector System Overlap. For nuclear weapons effects simulations, the array of open and closed detection channels is designed to have overlapping response functions to reduce calibration and measurement errors. The k-edges defining the response regions of the seventeen detectors used in this study are listed in Table 1. The k-edges are ratios computed with respect to  $E_1^0$ . The overlap of closed response functions is shown in Figure 3 (instruments 1-11 are shown left to right). Figure 4 shows the response functions for the collection of open detection systems (instruments 1-6 are shown left to right). Note that the open response detector systems completely overlap those of the closed response systems.

Table 1. Detector K-Edge Ratios

Detector #	$E_i^0$		Detector #	$E_i^0$	$E_i^1$
Open - 1	1		Closed - 1	1	2
Open - 2	2		Closed - 2	$\sqrt{2}$	$2\sqrt{2}$
Open - 3	4		Closed - 3	2	4
Open - 4	8		Closed - 4	$2\sqrt{2}$	$4\sqrt{2}$
Open - 5	16		Closed - 5	4	8
Open - 6	32		Closed - 6	$4\sqrt{2}$	$8\sqrt{2}$
			Closed - 7	8	16
			Closed - 8	$8\sqrt{2}$	$16\sqrt{2}$
			Closed - 9	16	32
			Closed - 10	$16\sqrt{2}$	$32\sqrt{2}$
			Closed - 11	32	64

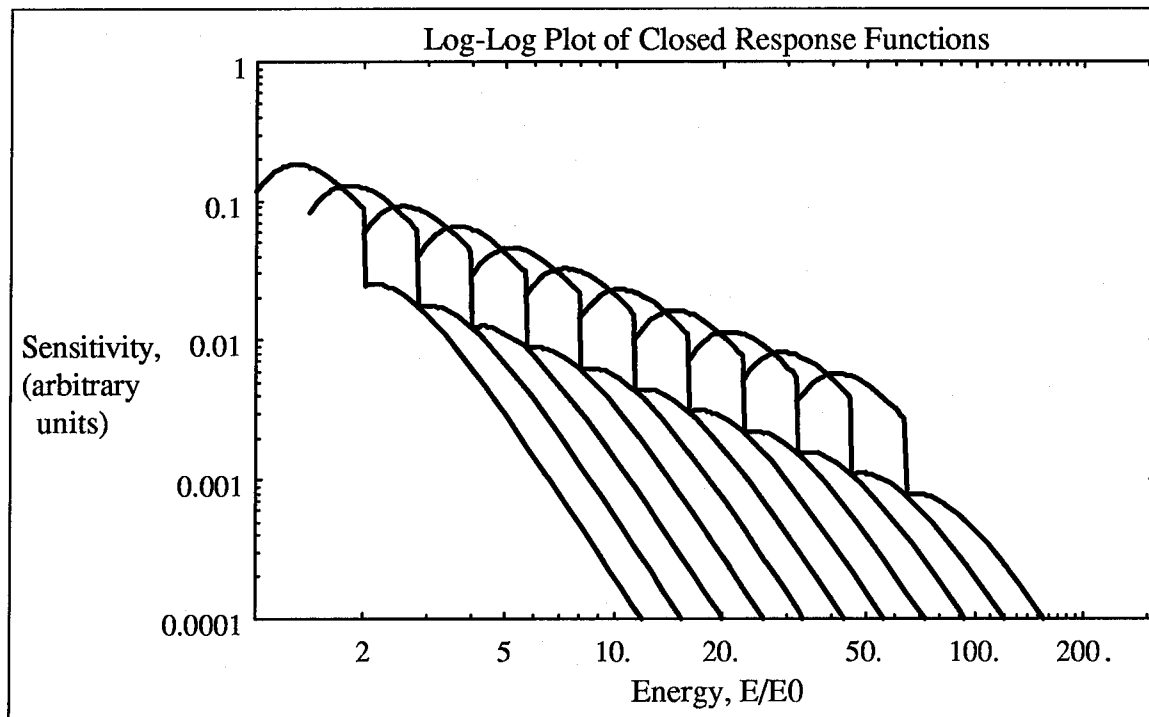


Figure 3. Closed Response Functions, Instruments 1-11

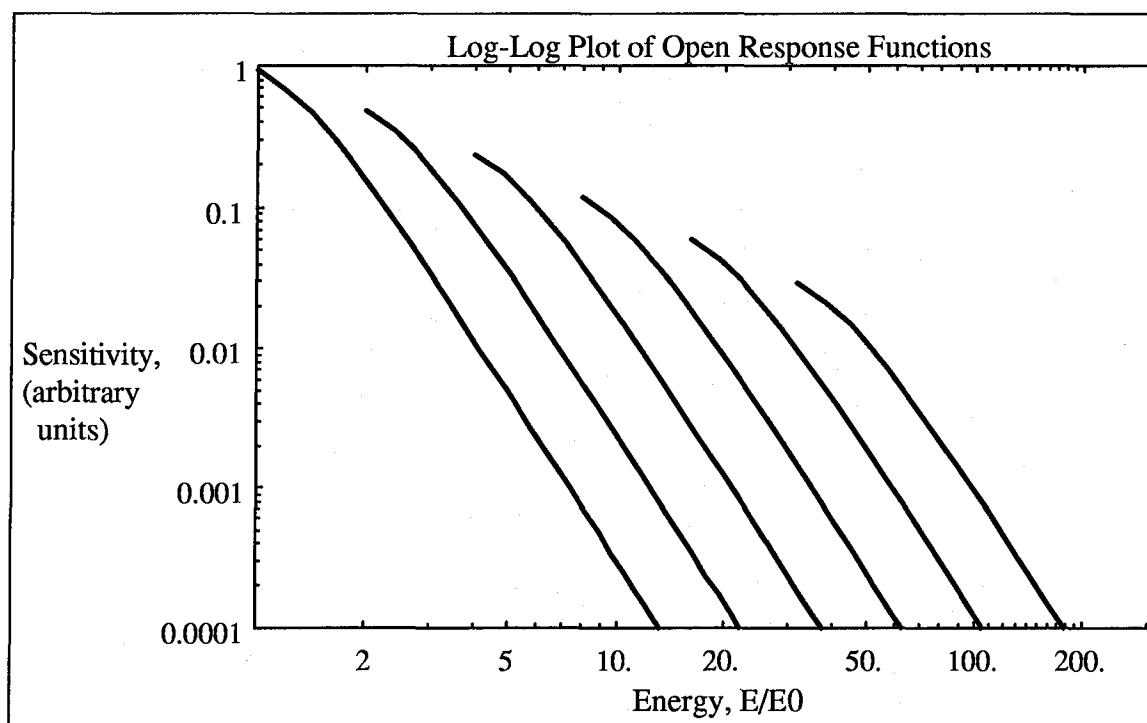


Figure 4. Open Response Functions, Instruments 12-17

Signal Detection. Practical aspects of data collection force several limitations on a detection system. These limitations include use of a finite number of detectors, limited detector resolution, and errors due to recording, transmitting and calibrating. As discussed above, pulsed radiation detection is accomplished using a series of overlapping detectors covering the energy range of interest. From Eq (4), the measured signal from each detector due to the total spectrum is represented by

$$\tilde{Y}_i = \int_0^{\infty} \tilde{S}(E) \tilde{R}_i(E) dE \quad (7)$$

where

$\tilde{Y}_i$  = the ideal signal of the  $i^{\text{th}}$  detector



$\tilde{S}(E)$  = the exact or actual spectrum emitted

$\tilde{R}_i(E)$  = the actual response of the  $i^{\text{th}}$  detector

In practice, multiple energy groups are used to numerically approximate integrals. This technique sums over small energy groups (bins) -- in essence, a composite numerical quadrature (Burden and Faires, 1993:Ch 4). Using the multi-group approach Eq (7) is:

$$\tilde{Y}_i \approx \sum_{j=1}^N \tilde{S}(E_j) \tilde{R}_i(E_j) \Delta E_j \quad (8)$$

where

$\tilde{S}(E_j)$  = the exact spectrum value for the  $j^{\text{th}}$  energy group

$\Delta E_j$  = the width of the  $j^{\text{th}}$  energy group

$N$  = the number of energy groups

### Sources of Error

Two main sources of error contribute to uncertainties in the spectrum and signals: measurement error (including transmission, recording and reading of the ideal signals) and errors due to the numeric approximation of integrals.

To reduce measurement error, overlapping detector response functions are used. In addition, two detector systems are employed. The analyst accounts for these errors by specifying a measurement standard deviation for each detector. These deviations are based on past experiments and detector calibrations. Measurement and calibration errors

associated with the detection system can be handled theoretically by applying normally distributed random noise to simulated measured signals (Carter, 1989:14-15).

The second error source is in the mathematical process, (i.e., the evaluation of the integrals equations via numeric quadrature). In this case, the approximation of the integral equation by a summation of discrete values, as in Eq (8), leads to approximation errors. These errors can be made negligible compared with other errors by selecting small bin widths in the summation process. Relative errors associated with the number of geometrically spaced bins used in the integral approximation are listed in Table 2.

Table 2. Relative Error Due to Numeric Approximation of Integral

	15 BINS	30 BINS	60 BINS	120 BINS
Instrument				
Closed #1	0.1193	0.0046	0.0011	0.0003
Closed #8	0.5008	0.4244	0.0042	0.0010
Open #1	0.0066	0.0016	0.0004	0.0001
Open #4	1.0198	0.0298	0.0075	0.0019
Target Loading	0.0040	0.0010	0.0003	0.0001

#### Preliminary Derivation

The through-fold process allows calculation of bounds for the target loading without intermediate calculation of the incident spectrum. This is accomplished by assuming exact target loading can be represented by a combination of known, predicted and bounded terms. Bounds on target loading are subsequently expressed as linear programming problems. The key is to develop a suitable target loading representation.

Definition of Exact Values. Throughout this section, the terminology will remain consistent with that presented earlier. Summarizing the nomenclature:

$\sim$	=	tilde, denotes an exact quantity, as opposed to measured
$\delta$	=	delta, denotes correction term determined from measurement error, calibration error, or a conservative estimate
$R_i(E)$	=	instrument response as a function of energy, $i^{\text{th}}$ instrument
$S(E)$	=	spectrum as a function of energy
$T(E)$	=	target response as a function of energy
$Y_i$	=	instrument signal, $i^{\text{th}}$ instrument
$Z$	=	target loading

NOTE: The absence of both tilde and delta indicates the quantity is measured or calibrated.

The derivation begins with a definition of target loading. Target loading can be viewed as the signal which would have been recorded by the target had it actually been an error free instrument. Target loading is thus represented similarly to instrument signal by:

$$\tilde{Z} = \int_0^{\infty} \tilde{S}(E) \tilde{T}(E) dE \quad (9)$$

None of the values in Eq (9) are actually known. Each can, however, be approximated by a measured or predicted value plus a correction term. If the target response function is further approximated as a linear combination of instrument responses plus a remainder, to

keep the relationship exact, then all the terms on the right hand side of Eq (9) can be replaced with known, predicted, or boundable values. Defining pertinent exact terms,

$$\tilde{S}(E) = S(E) + \delta S(E) \quad (10a)$$

$$\tilde{T}(E) = T(E) + \delta T(E) \quad (10b)$$

$$\tilde{R}_i(E) = R_i(E) + \delta R(E) \quad (10c)$$

$$\tilde{Y}_i = Y_i + \delta Y_i \quad (10d)$$

Equations (10) should be read as ‘the exact value equals a measured (or predicted) value plus a correction term’. The correction terms are not known since the exact values are unknown; however, they can be bounded. The four correction terms in Eqs (10) can be based on conservative estimates, calibration error, or measurement. An examination of the approximate magnitudes of these correction terms will help simplify the derivation.

Estimation of Error Bounds. The exact correction terms significantly influence the solution. Although the analyst has *a priori* information and possibly unfolded spectra to use in his spectrum prediction, the ill-posed problem dictates a conservative bound be placed on the spectrum correction,  $\delta S$ . For example, this bound could be  $\pm 50\%$  or even  $\pm 100\%$ .

Measurement error,  $\delta Y$ , consists of uncertainties in the measured detector output. This study considers the cumulative error related to data collection as measurement error. Although using two types of detector response functions helps minimize the measurement

error, its magnitude is still significant. This study assumes bounds on  $\delta Y$  to be  $\pm 15\%$ . This is consistent with previous work by Miller (1990), Carter(1989), and Daniel (1988).

The calibration error associated with the instruments,  $\delta R$ , is distinct from measurement error. Calibration error is an inherent uncertainty in the detector response function. The experimenter minimizes the magnitude of  $\delta R$  by calibrating the detection system. This study assumes calibration error is  $\pm 1\%$  to  $\pm 3\%$ .

Finally, there is uncertainty in the target response function,  $\delta T$ . The inability to directly calibrate the target would appear to dictate a conservative estimate for  $\delta T$ . However, this study will only consider well characterized target response functions.

Accepting the above magnitudes for the correction terms, a simplifying assumption concerning correction terms is made. For the remainder of the preliminary derivation, the magnitudes of  $\delta T$  and  $\delta R$  are considered negligible compared to  $\delta Y$  and  $\delta S$  and assumed equal to zero.

Development of Target Loading. As mentioned in Chapter I, the key idea of the through-fold technique is that the target response function can be represented as a linear combination of instrument response functions and a remainder. This approach provides the vehicle for incorporation of test data into the through-fold equations. The motive behind this approximation is best illustrated through several examples.

Motivation. By inspection of Eqs (9) and (10) it becomes obvious that exact target loading is driven by the large spectrum correction,  $\delta S$ . If the dependence on  $\delta S$  can be diminished (via incorporation of test data) then  $\tilde{Z}$  may have tighter bounds.

Suppose the exact target response is the sum of two exact instrument responses:

$$\tilde{T}(E) = \tilde{R}_6(E) + \tilde{R}_7(E) \quad (11)$$

By Eq (9), exact target loading is equal to the exact target response folded with the exact spectrum. Using this definition and Eq (11),  $\tilde{Z}$  reduces to the combination of exact instrument signals shown by the following steps:

$$\begin{aligned} \tilde{Z} &= \int \tilde{S}(E) \tilde{T}(E) dE \\ &= \int \tilde{S}(E) (\tilde{R}_6(E) + \tilde{R}_7(E)) dE \\ &= \int \tilde{S}(E) \tilde{R}_6(E) dE + \int \tilde{S}(E) \tilde{R}_7(E) dE \\ &= \tilde{Y}_6 + \tilde{Y}_7 \end{aligned} \quad (12)$$

The exact spectrum has now been replaced by the exact signal, which can be approximated using test data, measured signals, for  $Y_i$  in Eq (10d).

Next suppose that the exact target loading can be represented by a linear combination of the exact response of all the instruments,

$$\tilde{T}(E) = \sum_i a_i \tilde{R}_i(E) \quad (13)$$

where the  $a_i$ 's are coefficients for the  $i$  instruments. The  $a_i$ 's can be positive, negative, or zero. Again, exact target loading reduces to a linear combination of response functions:

$$\begin{aligned}
 \tilde{Z} &= \int \tilde{S}(E) \tilde{T}(E) dE \\
 &= \int \tilde{S}(E) \left( \sum_i a_i \tilde{R}_i(E) \right) dE \\
 &= \sum_i a_i \int \tilde{S}(E) \tilde{R}_i(E) dE \\
 &= \sum_i a_i \tilde{Y}_i
 \end{aligned} \tag{14}$$

Finally, suppose that  $\tilde{T}(E)$  is not quite a linear combination of exact instrument responses, but has a remainder term associated with it:

$$\tilde{T}(E) = \sum_i a_i \tilde{R}_i(E) + \tilde{T}_{\bar{a}}(E) \tag{15}$$

where  $\tilde{T}_{\bar{a}}(E)$  is the remainder term parametrically dependent on the choice of coefficients.

The expression for exact target loading now becomes:

$$\begin{aligned}
 \tilde{Z} &= \int \tilde{S}(E) \tilde{T}(E) dE \\
 &= \int \tilde{S}(E) \left( \sum_i a_i \tilde{R}_i(E) + \tilde{T}_{\bar{a}}(E) \right) dE \\
 &= \sum_i a_i \int \tilde{S}(E) \tilde{R}_i(E) dE + \int \tilde{S}(E) \tilde{T}_{\bar{a}}(E) dE \\
 &= \sum_i a_i \tilde{Y}_i + \int \tilde{S}(E) \tilde{T}_{\bar{a}}(E) dE
 \end{aligned} \tag{16}$$

Although not leading to an immediate solution, these examples provide insight into the form of the target response function approximation. The benefit from this approximation is the conversion of the exact spectrum to the exact instrument responses, which allows for the introduction of test data into the through-fold equations. One obvious complication is the addition of another unknown exact value,  $\tilde{T}_{\tilde{a}}(E)$ . However, proper selection of the  $a_i$  will result in a  $\tilde{T}_{\tilde{a}}(E)$  which will tighten (optimize) the overall bound on  $\tilde{Z}$ . Conversely, a poor choice of  $a_i$  will force a value for  $\tilde{T}_{\tilde{a}}(E)$  which will relax the overall bound on  $\tilde{Z}$ .

Derivation. Since terms on the right hand sides (RHS) of Eqs (10) are considered known, they can be substituted into the exact target loading equation, eliminating the unknowns. Substituting Eq (10b) into Eq (9) yields

$$\tilde{Z} = \int_0^{\infty} \tilde{S}(E) [T(E) + \delta T(E)] dE \quad (17)$$

Neglecting  $\delta T$  (for now):

$$\tilde{Z} = \int_0^{\infty} \tilde{S}(E) T(E) dE \quad (18)$$

It now becomes beneficial to introduce an approximation for  $T(E)$ . Note that the replacement is for  $T(E)$  and not  $\tilde{T}(E)$  as it was in the Motivation section. Hence the additional exact term from there will not complicate the derivation.



Approximating  $T(E)$  by a linear combination of instrument response functions and then making the relationship exact by carrying a remainder term yields the following:

$$T(E) = \sum_i a_i R_i(E) + T_{\bar{a}}(E) \quad (19)$$

where

$a_i$  = a constant for the  $i^{\text{th}}$  instrument

$T_{\bar{a}}(E)$  = a remainder based on the choice of  $a_i$ , defined by Eq (19)

Substituting the last equation into the expression for exact target loading and expanding,

$$\tilde{Z} = \sum_i a_i \int_0^{\infty} \tilde{S}(E) R_i(E) dE + \int_0^{\infty} \tilde{S}(E) T_{\bar{a}}(E) dE \quad (20)$$

Since  $\delta R$  has been assumed zero,  $R_i(E)$  can be replaced with  $\tilde{R}_i(E)$ . By also

approximating the exact spectrum with its approximation from Eq (10d),  $\tilde{Z}$  becomes

$$\begin{aligned} \tilde{Z} &= \sum_i a_i \int_0^{\infty} \tilde{S}(E) \tilde{R}_i(E) dE + \left[ \int_0^{\infty} S(E) T_{\bar{a}}(E) dE + \int_0^{\infty} \delta S(E) T_{\bar{a}}(E) dE \right] \\ &= \sum_i a_i \tilde{Y} + \int_0^{\infty} S(E) T_{\bar{a}}(E) dE + \int_0^{\infty} \delta S(E) T_{\bar{a}}(E) dE \end{aligned} \quad (21)$$

The importance of the derivation being performed in the order shown by Eqs (17) to (21) is to manipulate Eq (9) into the correct form for introduction of the exact instrument

signals,  $\tilde{Y}$ . Experimental data (measured signals) can now be explicitly introduced by approximating the exact signal using Eq (10d)

$$\tilde{Z} = \sum_i a_i Y_i + \sum_i a_i \delta Y_i + \int_0^\infty S(E) T_{\tilde{a}}(E) dE + \int_0^\infty \delta S(E) T_{\tilde{a}}(E) dE \quad (22)$$

The final expression for target loading is found by writing the above equation explicitly in terms of the  $a_i$  by replacing  $T_{\tilde{a}}(E)$  with its value from Eq (19).

$$\begin{aligned} \tilde{Z} = & \sum_i a_i Y_i + \sum_i a_i \delta Y_i \\ & + \int_0^\infty S(E) \left[ T(E) - \sum_j a_j R_j(E) \right] dE \\ & + \int_0^\infty \delta S(E) \left[ T(E) - \sum_j a_j R_j(E) \right] dE \end{aligned} \quad (23)$$

After simplifying and reversing the order of integration and summation,

$$\begin{aligned} \tilde{Z} = & \sum_i a_i Y_i + \sum_i a_i \delta Y_i \\ & - \sum_i a_i \int_0^\infty S(E) R_i(E) dE - \sum_i a_i \int_0^\infty \delta S(E) R_i(E) dE \\ & + \int_0^\infty S(E) T(E) dE + \int_0^\infty \delta S(E) T(E) dE \end{aligned} \quad (24)$$

Having the final analytic expression for the target loading, and bounds on the correction terms, Eq (24) must now be converted to a numeric one.

### Conversion to a Numeric Solution. Numeric computational concerns

dictate that the integrals in Eq (24) be approximated using a summation of terms over bins covering the full range of energy. An example of this multi-group approach was shown in Eq (8). Using the approximation from Eq (8),  $\tilde{Z}$  becomes

$$\begin{aligned} \tilde{Z} = & \sum_i a_i Y_i + \sum_i a_i \delta Y_i \\ & - \sum_i a_i \sum_{j=1}^N S(E_j) R_i(E_j) \Delta E_j - \sum_i a_i \sum_{j=1}^N \delta S(E_j) R_i(E_j) \Delta E_j \\ & + \sum_{j=1}^N S(E_j) T(E_j) \Delta E_j + \sum_{j=1}^N \delta S(E_j) T(E_j) \Delta E_j \end{aligned} \quad (25)$$

To make calculations easier, it is beneficial to define an instrument response matrix,  $\mathbf{R}$ , a spectrum vector,  $\mathbf{s}$ , an instrument signal vector,  $\mathbf{y}$ , a target response vector,  $\mathbf{t}$ , and a constant  $a_i$  vector,  $\mathbf{a}$ , as

$$\begin{aligned} (\mathbf{R})_{ij} &= R_i(E_j) \Delta E_j \\ (\mathbf{s})_j &= S(E_j) \\ (\mathbf{y})_i &= Y_i \\ (\mathbf{t})_j &= T(E_j) \Delta E_j \\ (\mathbf{a})_i &= a_i \end{aligned} \quad (26)$$

Now converting the exact target loading into vector notation (detailed in Appendix A):

$$\begin{aligned}\tilde{Z} = & \mathbf{a} \cdot (\mathbf{y} + \delta \mathbf{y} - \mathbf{R} \cdot \mathbf{s} - \mathbf{R} \cdot \delta \mathbf{s}) \\ & + \mathbf{s} \cdot \mathbf{t} + \delta \mathbf{s} \cdot \mathbf{t}\end{aligned}\quad (27)$$

Equation (27) is an exact expression for target loading because the exact correction vectors,  $\delta \mathbf{s}$  and  $\delta \mathbf{y}$ , have been carried throughout the derivation. Unfortunately, Eq (27) can not be computed because the exact delta values are unknown.

Bounds on Exact Target Loading. The value of  $\tilde{Z}$  given by Eq (27) cannot be calculated because the delta terms are not known exactly, only within the bounds on the correction terms discussed previously. The exact target loading can be bound by

$$Z^L \leq \tilde{Z} \leq Z^U \quad (28)$$

where  $Z^U$  and  $Z^L$  are the upper and lower bounds respectively on target loading.

The upper (or lower) target loading bounds defined above can be computed for any fixed choice of  $\mathbf{a}$  by choosing the values for  $\delta \mathbf{s}$  and  $\delta \mathbf{y}$  -- both being allowed to vary (within the error bounds) at each energy bin -- to maximize (or minimize) the target loading expression, which is implicitly a function of  $\mathbf{a}$ . These bounds are computed by solving the following linear programs for the upper and lower target loading bounds respectively:

$$\begin{aligned}Z^U(\mathbf{a}) &= \text{Max}_{\delta \mathbf{y}, \delta \mathbf{s}} [\mathbf{a} \cdot (\mathbf{y} + \delta \mathbf{y} - \mathbf{R} \cdot \mathbf{s} - \mathbf{R} \cdot \delta \mathbf{s}) + \mathbf{s} \cdot \mathbf{t} + \delta \mathbf{s} \cdot \mathbf{t}] \\ Z^L(\mathbf{a}) &= \text{Min}_{\delta \mathbf{y}, \delta \mathbf{s}} [\mathbf{a} \cdot (\mathbf{y} + \delta \mathbf{y} - \mathbf{R} \cdot \mathbf{s} - \mathbf{R} \cdot \delta \mathbf{s}) + \mathbf{s} \cdot \mathbf{t} + \delta \mathbf{s} \cdot \mathbf{t}]\end{aligned}\quad (29)$$

In Eq (29)  $\delta y$  and  $\delta s$  are variables subject to the following constraints

$$\begin{aligned}\delta y_{\min} &\leq \delta y \leq \delta y_{\max} \\ \delta s_{\min} &\leq \delta s \leq \delta s_{\max}\end{aligned}\tag{30}$$

$R$ ,  $s$ ,  $t$ , and  $y$  are input data; and  $a$  is the variable for which the bound is to be determined.

The goal functions of both bounds in Eq (29) are the same and are given by:

$$f(\delta y, \delta s) = a \cdot (y + \delta y - R \cdot s - R \cdot \delta s) + s \cdot t + \delta s \cdot t \tag{31}$$

The upper bound is found by maximizing the goal function over  $\delta y$  and  $\delta s$ . Similarly, the lower bound is found by minimizing the goal function over the  $\delta y$  and  $\delta s$ . The resulting values for  $Z^U(a)$  and  $Z^L(a)$  from Eq (29) represent the largest possible values of  $Z$  (maximum and minimum respectively) on target loading for fixed set of  $a$ . However, it should be possible to tighten these bounds by selecting appropriate sets of  $a$ . The process of selecting the  $a$ 's resulting in the tightest possible bounds is accomplished by optimizing the upper and lower bound over all possible choices of  $a$ . The result is a classic minimum-maximum (mini-max) problem given by:

$$\begin{aligned}Z_{\min}^U &= \underset{a}{\text{Min}} [Z^U(a)] \\ Z_{\max}^L &= \underset{a}{\text{Max}} [Z^L(a)]\end{aligned}\tag{32}$$

$Z_{\min}^U$  is the minimum upper bound (least upper bound) for target loading and is found by minimizing  $Z^U(\mathbf{a})$  over  $\mathbf{a}$ .  $Z_{\max}^L$  is the maximum lower bound for target loading, found by maximizing  $Z^L(\mathbf{a})$  over  $\mathbf{a}$ . The outer loop of the mini-max problem is an unconstrained (the  $\mathbf{a}$  vector can take on any values) optimization problem.

Standard Form. The goal function in Eq (31) can not directly be used in a linear programming problem because it is not in standard form. The standard form for linear programming problems requires non-negative variables. The bounded error terms are therefore defined as the difference of two positive numbers

$$\begin{aligned}\delta Y &= \delta Y^+ - \delta Y^- \\ \delta S &= \delta S^+ - \delta S^-\end{aligned}\tag{33}$$

where all the terms on the RHS of Eq (33) are greater than or equal to zero.

The inner loops of the mini-max problems will force one of the terms on the RHS of Eq (33) to zero and the other to its maximum magnitude at each energy bin. The first term will be zero if the worst case error is negative while the second term will be zero if the worst case error is positive. Inserting the non-negativity constraints into Eq (31), the goal function to be maximized and minimized becomes

$$\begin{aligned}f(\delta y, \delta s) = \mathbf{a} \cdot & \left[ \mathbf{y} + \delta y^+ - \delta y^- - \mathbf{R} \cdot \mathbf{s} - \mathbf{R} \cdot \delta s^+ + \mathbf{R} \cdot \delta s^- \right] \\ & + \mathbf{s} \cdot \mathbf{t} + \delta s^+ \cdot \mathbf{t} - \delta s^- \cdot \mathbf{t}\end{aligned}\tag{34}$$

subject to the following constraints

$$\begin{aligned}
0 &\leq \delta y^+ \leq \delta y_{\max} \\
0 &\leq \delta y^- \leq |-\delta y_{\min}| \\
0 &\leq \delta s^+ \leq \delta s_{\max} \\
0 &\leq \delta s^- \leq |-\delta s_{\min}|
\end{aligned}
\tag{35}$$

The goal function of Eq (34) remains linear in the delta terms (as is the analytic solution).

The linearity of the goal function lends itself to a number of optimization routines. It should be pointed out that this method is much more generally applicable than as used here. As a point of fact, the delta terms ( $\delta y_{\max}$ ,  $\delta y_{\min}$ ,  $\delta s_{\max}$ , and  $\delta s_{\min}$ ) need not be constants (e.g., +15%, -15%, +50%, and -50%), but can vary in magnitude with the energy bins.

#### Differences In The Full Derivation

The preliminary derivation assumed instrument calibration errors and target calibration errors were negligible. However, they are not zero and must be included in a formal derivation of  $\tilde{Z}$ . Appendix A contains a formal derivation of exact target loading. This section highlights the main differences in preliminary and formal derivations.

Processes associated with the formal derivation are similar to those found in the preliminary derivation; therefore, the full analytic solution appears similar to the shorter exact target loading expression from Eq (24). The full analytic solution is

$$\begin{aligned}
\tilde{Z} = & \sum_i a_i Y_i + \sum_i a_i \delta Y_i \\
& - \sum_i a_i \int_0^\infty S(E) R_i(E) dE - \sum_i a_i \int_0^\infty \delta S(E) R_i(E) dE \\
& - \sum_i a_i \int_0^\infty S(E) \delta R_i(E) dE - \sum_i a_i \int_0^\infty \delta S(E) \delta R_i(E) dE \quad (36) \\
& + \int_0^\infty S(E) T(E) dE + \int_0^\infty \delta S(E) T(E) dE \\
& + \int_0^\infty S(E) \delta T(E) dE + \int_0^\infty \delta S(E) \delta T(E) dE
\end{aligned}$$

One difference between the two derivations is that four new integrals containing two additional error terms,  $\delta R_i(E)$  and  $\delta T(E)$ , appear in Eq (36). The presence of the additional terms do not in themselves change the overall technique for finding a solution. A more significant difference between the two expressions is that two of the integrals now contain more than one correction term. This second difference results in bounds on  $\tilde{Z}$  changing from linear programming problems to quadratic programming problems.

The non-linearity of  $\tilde{Z}$  is easily seen in the numerical approximation of Eq (36):

$$\begin{aligned}
\tilde{Z} = & \mathbf{a} \cdot \left\{ \begin{array}{l} \mathbf{y} + \delta \mathbf{y} - \mathbf{R} \cdot \mathbf{s} - \mathbf{R} \cdot \delta \mathbf{s} \\ - \delta \mathbf{R} \cdot \mathbf{s} - \delta \mathbf{R} \cdot \delta \mathbf{s} \end{array} \right\} \quad (37) \\
& + \mathbf{s} \cdot \mathbf{t} + \delta \mathbf{s} \cdot \mathbf{t} + \mathbf{s} \cdot \delta \mathbf{t} + \delta \mathbf{s} \cdot \delta \mathbf{t}
\end{aligned}$$

This quadratic equation is much more difficult to solve than the simplified linear equation. The remainder of this study considers only linear dependence on error terms.



### Through-fold Expectations

The through-fold method is beneficial only if it produces tighter bounds than can be calculated based on estimated error bounds. As discussed under Motivation, how well the method works depends on the choice of  $a_i$ . A good choice of  $a_i$  will result in a value for  $T_{\tilde{a}}(E)$  which tighten bounds on  $\tilde{Z}$ . Conversely, a poor choice of  $a_i$  could result in large bounds on  $\tilde{Z}$ . Since  $T_{\tilde{a}}(E)$  is a remnant of the through-fold method, it can be viewed as error (the correction) associated purely with the technique. How well through-fold performs is therefore linked to how well  $T_{\tilde{a}}(E)$  is optimized. Optimization over  $\mathbf{a}$  does not mean minimization of  $T_{\tilde{a}}(E)$ , but in choosing  $T_{\tilde{a}}(E)$  to tighten bounds on  $\tilde{Z}$ .

Conservative Estimate. A conservative estimate on the exact target loading error bounds can be calculated prior to performing an experiment. This error would be based solely on propagation of expected errors. By utilizing the inner loop of through-folds' mini-max routines, the conservative value can be calculated. This is done by computing  $Z^L(\mathbf{a})$  and  $Z^U(\mathbf{a})$  with all  $a_i$  set to zero, eliminating instrument influence on the solution. How accurately through-fold techniques calculate the conservative value depends on the number of bins used in the numerical integration.

Introduction of Experimental Data. The introduction of experimental data into the through-fold routines will help optimize  $T_{\tilde{a}}(E)$  and therefore tighten bounds on the exact target loading. The reason for this is seen by comparison of two equations. The first

equation is found from a naive approach to the original exact target loading expression, Eq (9). Starting with Eq (9) and remembering  $\delta T(E)$  has been defined as zero yields:

$$\begin{aligned}
 \tilde{Z} &= \int_0^{\infty} \tilde{S}(E) \tilde{T}(E) dE \\
 &= \int_0^{\infty} \tilde{S}(E) T(E) dE \\
 &= \int_0^{\infty} [S(E) + \delta S(E)] T(E) dE \\
 &= \int_0^{\infty} [S(E) T(E) dE] + \int_0^{\infty} [\delta S(E) T(E) dE]
 \end{aligned} \tag{9b}$$

The second equation is  $\tilde{Z}$  prior to simplification, a variation of Eq (22):

$$\begin{aligned}
 \tilde{Z} &= \sum_i a_i Y_i + \sum_i a_i \delta Y_i + \int_0^{\infty} S(E) T_{\tilde{a}}(E) dE + \int_0^{\infty} \delta S(E) T_{\tilde{a}}(E) dE \\
 &= \sum_i a_i Y_i + \sum_i a_i \delta Y_i + \int_0^{\infty} \tilde{S}(E) T_{\tilde{a}}(E) dE
 \end{aligned} \tag{22b}$$

As seen by Eqs (9b) and (22b), the only error associated with the naive approach is the *a priori* spectrum error (estimated at  $\pm 50\%$ ). After applying through-fold techniques the spectrum error is replaced with measurement error (estimated at  $\pm 15\%$ ) propagating into the choice of  $a$  plus the error associated with the through-fold method,  $T_{\tilde{a}}(E)$ , propagating into the exact spectrum. As discussed previously, the proper choice of  $a_i$  will

optimize  $T_{\vec{a}}(E)$ . If  $T_{\vec{a}}(E)$  is driven towards zero, then the resulting error is driven towards the measurement error (assuming propagation of measurement error is not significant). However, if  $T_{\vec{a}}(E)$  can not be driven low enough, additional error associated with the integral will counteract some, or even all, of the difference between  $\delta S$  and  $\delta Y$ .

It is important to realize that the optimal  $T_{\vec{a}}(E)$  may not always be the minimum. If all  $a_i$  are found to be positive, or all negative, then propagation of the measurement errors will be such that the optimal  $T_{\vec{a}}(E)$  is as small as possible. However, if the sign of the  $a_i$  vary, then propagation of measurement errors may dictate that the optimal  $T_{\vec{a}}(E)$  not be its minimum.

Incrementing Experimental Data. As the number of instruments used in the through-fold increases, the error bounds are expected to tighten. This occurs because the additional test data more accurately define the incident spectrum implicitly contained in the instrument measurements. But more importantly, with the addition of each instrument, the routine is given two additional degrees of freedom for determining the  $a_i$ . The theoretical minimum error bound is equal to the measurement error; however, it is unlikely that this minimum will be reached.

There are two primary reasons that the optimized error bound is not expected to reach the theoretical minimum error bound. First, as discussed previously, all the  $a_i$  are not necessarily the same sign. Second, the target response function is not a linear combination of the instrument response functions.

### III. Computer Implementation

#### Introduction

Chapter II provided the theoretical background for understanding the through-fold concept. This section covers implementation of the through-fold equations. Included in this discussion are the implementation platform, input data, error considerations, optimization routines, and the final computer code.

#### Platform

The computer program *Mathematica*, ran on a personal computer, was chosen for through-fold implementation. Along with modest built-in optimization routines and the capability to handle the vector equations from Chapter II, *Mathematica's* notebook interface allows creation of interactive files for future use.

#### Input Data

As discussed in Chapter II, a variety of input data is required to perform a linear optimization of Eq (34). The data normally available to the analyst from theoretical treatment of the physics and from past tests will be simulated. This includes the *a priori* spectrum and instrument response functions, the target response function, and all associated error. This section will define the data used for the original validation of the method. Instrument response functions and required errors were defined in Chapter II.

Spectrum. A continuous normalized Planckian spectrum was chosen to simulate the incident spectrum. The equation for a one temperature Planckian spectrum is

$$S(E) = sf \left( \frac{15}{kT \pi^4} \right) \frac{\left( \frac{E}{kT} \right)^3}{\exp\left(\frac{E}{kT} - 1\right)} \quad (38)$$

where  $E$  is energy,  $kT$  is the temperature of the radiation spectrum (units of  $E_1^0$ ), and  $sf$  is a scaling factor for the radiation spectrum. A convenient single temperature validation spectrum ( $kT = 1E_1^0$ ) and scaling factor of one was chosen for validation. Figure 5 is a plot of the validation spectrum.

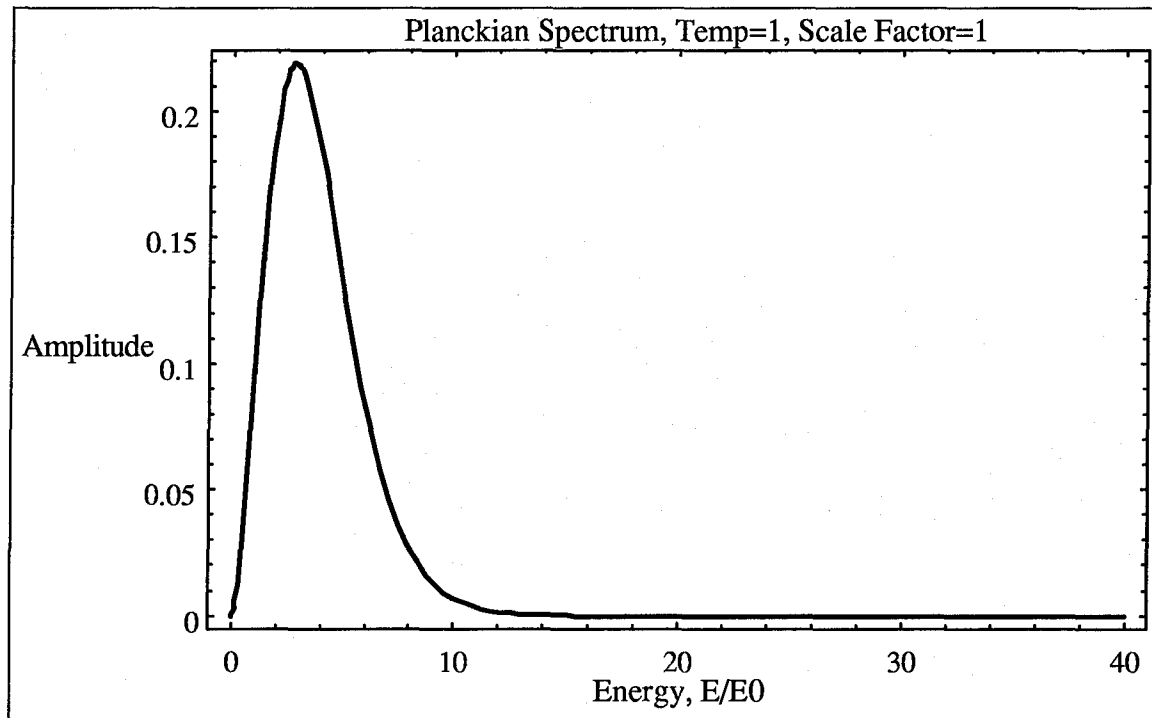


Figure 5. Validation Planckian Spectrum

Target Response Function. A Gaussian distribution function was chosen to approximate the target response function,  $T(E)$ , for the validation case. The equation for a Gaussian distribution is given by:

$$T(E) = \frac{1}{\sigma \sqrt{2\pi}} \exp \left[ -\frac{1}{2} \left( \frac{E - \mu}{\sigma} \right)^2 \right] \quad (39)$$

where  $E$  is energy,  $\mu$  is the mean of the distribution, and  $\sigma$  is the standard deviation of the distribution. A Gaussian distribution with a mean of zero and standard deviation of  $15 E_1^0$  was chosen for the validation target response function. The choice of test target response functions will be discussed Chapter IV. Figure 6 is a plot of the validation target response function.

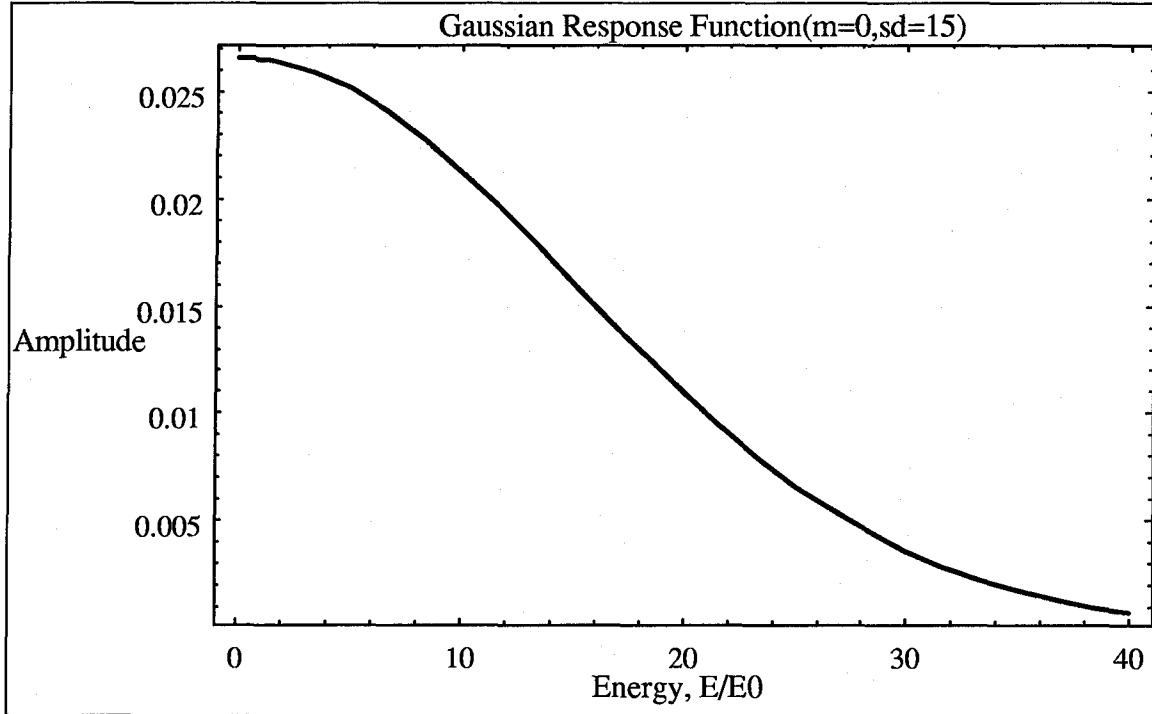


Figure 6. Validation Target Response Function

Instrument Signal. Exact instrument signals are constructed by folding the simulated spectrum with the detector response functions. The folding is accomplished via the numerical approximation of Eq (7) and by assuming that the *a priori* spectrum definition and calibrated instrument response functions are exact. Calculation of the exact signal is simplified in *Mathematica* by using the matrix and vector definitions from Eq (26). The exact signal can then be calculated by:

$$\tilde{Y} = \mathbf{R} \cdot \mathbf{S} \quad (40)$$

All matrix and vector functions from Eq (26) are evaluated at the geometric centers of geometrically spaced energy bins. Bin spacing and centers were chosen to correspond to the geometric spacing of the instrument response functions. Geometrically spaced bins result in the majority of bins (60%) within the first quarter of the energy range. Geometrically spaced energy bins are desirable for this application because of the higher resolution provided to the lower k-edge detection systems than is possible using linear bin spacing for the same computational costs (i.e., the same number of bins). The advantage is due to all the interesting details of the chosen incident spectrum, target response functions, and instrument response functions occurring at the lower energies. The *Mathematica* notebook allows for computation of linearly spaced bins with linear centers for cases having considerable detail at higher energies. Candidate test cases for linear spacing include high temperature Planckian spectra.

## Error Considerations

Numerical Approximation. Geometric energy bin spacing is used to reduce errors in approximating integrals with summations. As shown in Table 2, use of a 120 bin grid produces relative errors of less than  $10^{-3}$  in approximating the required integrals. To save computational costs, the validation cases used 30 bins, producing a relative error that varies with instrument as shown in Table 2. Unfortunately, the relative errors associated with the instruments increase from 0.001 to 0.42 as the fluorescer k-edge increases. The high relative error associated with closed instrument #8 would normally be unacceptable; however, the spectrum value associated with the operational energy range of this instrument ( $E > 11.5 E_1^0$ ) is approximately  $10^{-3}$ . Although the total signal generated by this instrument is highly uncertain, its magnitude is too small ( $10^{-5}$  compared to  $10^{-2}$  for lower numbered instruments) to significantly influence the through-fold results.

Noise Simulation. In calculating the exact instrument signals (Eq 39), the calibrated instrument response functions,  $R_i(E)$ , are assumed exact. However, the exact target loading equations in Chapter II require measured signals. This study simulates measurement error by the addition of random noise. These errors are assumed normally distributed and determined by randomly sampling a Gaussian probability distribution.

This error approximation was performed using a *Mathematica* statistical package. A single random value, based on the instrument's standard deviation, was selected from a normal distribution. In keeping with previous unfolding studies, the instrument standard deviation is taken to be 15% and includes the totality of measurement related errors.



## Optimization Routines

Built in *Mathematica* routines were used for the two step mini-max optimization discussed in Chapter II. The first routine requires maximizing and minimizing capabilities for the linear target loading function over the bounds on the error terms. *Mathematica* provides two vehicles (LinearProgramming, and ConstrainedMax /ConstrainedMin) for computation of global maxima and minima in linearly programming problems. The constrained commands were chosen because they easily implement variable sized problems and automatically calculate the constrained solution based on the optimal constraints.

The second optimization routine requires minimization of all possible maximum values and maximization of all possible minimum values to reduce the error band between the two cases. *Mathematica* provides a minimization routine for unconstrained problems. The command FindMinimum was used to optimize the solutions. The upper and lower bounds were allowed to use different sets of  $a_i$  to optimize the bound. See Appendix B for the complete *Mathematica* notebook implementing these commands.

Performance of optimization routines is often linked to the initial values provided as starting points to the program. This is a concern with *Mathematica*'s FindMinimum command as it is not guaranteed to return a global minimum value. As used with the through-fold equations, the FindMinimum command requires the input of the first two points from which to perform a search for a local minimum. A method of steepest descent on the surface (function) is used by the routine to find the minimum.

In development of through-fold a number of tests were performed to evaluate the sensitivity of the method to initial guesses. Although not performed in a systematic

manner, testing of initial values around (and away from) known minimums was conducted. The optimization routines were found to be relatively insensitive to variations in the starting values.

### ThruFold.ma

ThruFold.ma is the final version of the through-folding code. A printed copy of ThruFold.ma is provided at Attachment B. The computer code is a *Mathematica* for Windows version 2.2 notebook which optimizes bounds on exact target loading (linear dependence on error bounds only). The code is written in three sections: 1) selection of input data, 2) evaluation of vectors and matrixes and 3) optimization.

The first section allows the user to select from a number of incident spectra, target response functions, and error terms through evaluation of appropriate cells. The user is then allowed to select the number of instruments, number of bins, bin spacing (geometric or linear), energy range to be covered, and the fluorescer k-edge of the first detector. Finally the instrument response functions are defined. The second section of ThruFold.ma defines vectors for the exact and measured signals, spectrum, target responses, all error approximations, and the instrument response matrix. The final section of the notebook defines the exact target loading using the final form of the linear programming goal function, Eq (34), develops equations for maximum and minimum values, and provides examples for calculation of the final bounds. Default values fit the validation test case.

## IV Validation and Testing

### Introduction

In Chapter III the implementation of the through-fold methodology was discussed. In this Chapter the validation cases and test cases are presented and compared to the expectations from Chapter II.

### Validation

A validation case was constructed to ensure proper operation of the through-fold routine. There are two validation goals. The first validation goal is to ensure that through-fold produces the expected conservative error when all  $a_i$  are set to zero. The second goal is to verify that error bounds decreased incrementally as additional instruments were introduced to the through-fold.

Proper verification of the first goal involves comparing the through-fold results with the exact target loading. As mentioned in Chapter II, the accuracy of the results are dependent on the number of bins used to approximate the integrals. Comparisons will be complicated by this difference if not using a substantial number of bins. For comparison purposes only, a pseudo-exact target loading is assumed equal to the dot product between the spectrum and target loading vector. Vector dimensions are based on the number of bins used for a given test. This assumption alleviates numerical approximation error when all  $a_i$  are set equal to zero.

Validation Case. The input data for validation were defined in Chapter III to be a broad Gaussian target response function (mean = 0, standard deviation = 15), a one temperature Planckian spectrum (temperature =  $1 E_1^0$ , scaling factor = 1), and 30 geometrically spaced bins covering an energy range from  $1 E_1^0$  to  $64 E_1^0$ . Each geometrically spaced bin has a width ratio (upper edge to lower edge) equal to  $\sqrt{2}$ . Measurement error has been introduced to the exact signals necessitating the inclusion of them in the constrained optimization routines. The validation case uses three test data variations: 1) only closed instrument signals, 2) only open instrument data, and 3) signals from both closed and open instruments in the through-fold.

Validation Results. Results of the validation method are encouraging. All three variants determined the error computed when all  $a_i$  equal zero to be  $\pm 50\%$ . Table 3 lists the results (maximum and minimum bounds on exact target loading) from the first validation variant--only closed instrument signals. The instruments used in each test are chosen sequentially based on the lowest fluorescer k-edge (e.g., No. Insts. = 4 indicates the first four closed instruments (left to right) as shown in Figure 3).

Table 3. Validation Results (Bounds on Target Loading), Closed Instruments

No. Insts.	0	2	4	6	8	10	11
$Z_{\min}^U$	0.03696	0.03514	0.03971	0.03457	0.03452	0.03452	--
Pseudo Exact Z	0.02464	0.02464	0.02464	0.02464	0.02464	0.02464	0.02464
$Z_{\max}^L$	0.01232	0.01525	0.01849	0.02009	0.02046	0.02030	--
Upper Bound, % +	50.0	42.6	61.2	40.3	40.1	40.1	--
Lower Bound, % -	50.0	38.1	25.0	18.4	17.0	17.6	--

The bounds on target loading are shown as a percentage relative to the pseudo-exact target loading. The bounds generally decrease from the naively computed maximum of  $\pm 50\%$  with no instruments. It is interesting that the upper and lower bounds are not driven to the same value. This is expected as separate optimization of upper and lower bounds allow each to have its own set of  $a_i$  and hence different optimal values.

The optimization routines were unable to compute bounds when all eleven closed instruments were used. Although unfortunate, this is not unexpected due to the extremely small signals associated with the last few instruments. Figure 3 indicates the last closed instrument has a maximum response less than 0.01 at an energy of  $45 E_1^0$ . The spectrum value associated with this energy is  $\sim 10^{-16}$ . The *Mathematica* optimization routine could not handle the small variations associated with this instrument.

Table 3 clearly shows that the optimal maximum error bound increased beyond the naive value when computed using four instruments. This was unexpected as the routine should have performed no worse than when using two instruments. As a check of the expected insensitivity on the starting values provided to the FindMinimum command (see Chapter 3, Optimization Routines), further testing was performed on this anomaly.

In all 14 additional tests were run. The first five tests varied the starting values of all four instruments while the remaining tests concentrated on the starting location of only one instrument. Four of the first five tests resulted in relative upper bounds near 61%, supporting the previous conclusion, relative insensitivity to starting positions. The fifth test resulted in a bound of 32%, less than the naive case, as expected, but also less than other closed instrument upper bounds, this was unexpected and lead to additional testing.

The second set of nine tests varied only the starting locations of the fourth instrument. The fourth instrument was chosen because it was the only instrument for which initial values were changed when the 32% bound was achieved. Eight of these nine test found a relative bound near 32%. There does not appear to be a set pattern, but as long as one (1) was not used as the first of the two initial starting locations (both 0.5 and 1.5 work), then the minimum upper bound was less than 35%. The second of the two guesses did not appear to be a driver for the optimization routine.

These results indicate that there may be two local minima for the function. However, since starting values above and below one (1) can be chosen that result in a 32% bound, the two apparent minimum values may actually indicate a slowly varying minimum. Results from the additional testing indicate proper performance of the through-fold method requires user artisanship. However, the importance of the user involvement may only be a factor due to the limited capabilities of the minimization routine (a steepest decent method) utilized by the FindMinimum command.

Another possible cause for the observed erratic behavior is inadequate resolution of the instrument response functions as provided by the 30 bin structure. This type of inadequacy could result in some closed instruments becoming indistinguishable in their response from the open instruments responses. However, the exact cause for this anomaly remains unexplained beyond the non-robustness of the *Mathematica* kernel.

A final observation from validation case #1 is that the total relative bound reduced from a naive value of 100% to 57% (49% after additional testing) utilizing only closed instrument responses.

Validation results from the open instruments are listed in Table 4. The results are comparable to those for closed instruments. Naive error equals  $\pm 50\%$ , bounds decreased as instruments were added, and the minimization routine failed for the last instrument. Non-robustness of the optimization routines are again expected to be the culprit.

Table 4. Validation Results (Bonds on Target Loading), Open Instruments

No. Insts.	0	1	2	4	5	6
$Z_{\min}^U$	0.03696	0.03576	0.03131	0.02970	0.02970	0.02970
Pseudo Exact Z	0.02464	0.02464	0.02464	0.02464	0.02464	0.02464
$Z_{\max}^L$	0.01232	0.01332	0.01408	0.01639	0.01639	--
Upper Bound, %+	50.0	45.2	27.1	20.5	20.5	20.5
Lower Bound, %-	50.0	46.0	42.9	33.5	33.5	--

There are two differences between closed and open instruments results. First, the open responses correspond to tighter overall bounds than for closed instruments (53% compared to 57%). The tighter bounds are predominantly due to a large reduction of the upper bound. Second, the overall lower bound was optimized using closed instruments while the upper bound was optimized using the signals from open instruments. This last difference is consistent with allowing separate optimizations based on instrument type.

The third validation case, use of open and closed instrument responses in the through-fold failed. The optimization routines were unable to converge to a solution. Two possible reasons are inadequate bin spacing and hence insufficient instrument resolution and the non-robustness of the optimization routines. However, the routine

should have been capable of producing results no worse than the best combination of the two previous cases (i.e., an upper bound of  $\pm 20.5$  and a lower bound of  $\pm 17.5\%$ ).

With the exception of the anomaly observed in the 4-closed channel results, the validation test verified all expectations. Even though some limitations of the optimization routines were found, through proper selection of the  $a_i$  vector and prudent choice of instrument response systems used in the through-fold, the overall error bound was decreased from 100% to 38% by the through-fold technique. Remember the theoretical minimum was 30% in the validation cases due to the built-in  $\pm 15\%$  measurement error.

### Testing

A few changes were made to the optimization problem between the validation and test cases. In an effort to save computational time the number of bins was reduced to 20. In order to counteract the subsequent decrease in the accuracy of the numerical calculations, the energy range was decreased from 64 to 40 energy units. The resulting numerical approximation error was verified to be comparable to the original error using 30 bins (0.005 to 0.04 relative error -- with the exception of high numbered closed instruments). This strategy worked in reducing the error due to the two factors discussed previously, geometric bin spacing and the low spectrum values beyond energy unit  $15E_1^0$ .

Only 12 of the original 17 detector systems are used, eight closed and four open detection systems. There are two reasons for this change. First, by decreasing the energy range some instrument response functions fall predominantly outside the area of concern. Second, the validation (along with all other trials) resulted in the optimized error bounds



being reached prior to incorporation of the eighth closed and fourth open instrument. It was assumed that the test cases would behave in a similar manner as long as the target response function did not significantly increase (compared to the validation case) at energies above  $20E_1^0$ . Lastly, based on validation results from case 3, optimization was not performed using signals from open and closed detection systems simultaneously.

Test Cases. Three test cases were constructed to study the behavior of through-fold, specifically the influence of  $T_{\vec{a}}(E)$  on the solution. All three cases are based on a target response function that is a linear combination of instrument response functions. Since through-fold is designed to optimize bounds on target loading over the  $a_i$ , which define  $T_{\vec{a}}(E)$ , target response functions having specific  $T_{\vec{a}}(E)$  were chosen as test cases. Resulting optimized bounds and  $T_{\vec{a}}(E)$  are compared to the originally defined values. The first test case uses a linear combination of instrument response functions to define  $T(E)$  such that the remainder is zero. In test case 2,  $T(E)$  is defined as the same linear combination of response functions but  $T_{\vec{a}}(E)$  is defined as a positive correction outside the instrument response envelope. The third test case is similar to the preceding case except  $T_{\vec{a}}(E)$  is defined as a negative correction; the same  $T_{\vec{a}}(E)$  is subtracted from the linear combination instead of being added to it.

Based on validation results, four variations were performed on each test case. The first variation defined  $T(E)$  as a positive combination of closed instrument response functions. The second variation used a positive combination of open response functions. The third variation used positive combinations of both types of detection systems, the final

variation was not restricted to linear combinations of positive terms (i.e., the  $a_i$  can be negative). The selection of four combinations of instrument responses requires four  $T_{\bar{a}}(E)$  definitions. This stems from a non-negativity constraint on the target response function. The four linear combinations of instrument responses are listed below.

$$\text{Variation A:} \quad T(E) = R_1(E) + 2.5R_3(E) \quad (41a)$$

$$\text{Variation B:} \quad T(E) = R_9(E) + R_{11}(E) \quad (41b)$$

$$\text{Variation C:} \quad T(E) = R_1(E) + 2.5R_3(E) + R_9(E) + R_{11}(E) \quad (41c)$$

$$\text{Variation D:} \quad T(E) = 2 \begin{bmatrix} 1.2R_1(E) + 0.75R_3(E) - 1.75R_7(E) \\ -0.15R_8(E) + 0.5R_{11}(E) + R_{12}(E) \end{bmatrix} \quad (41d)$$

Figures 7-10 show  $T(E)$  and Figures 11-14 show the defined  $T_{\bar{a}}(E)$  for the test cases.

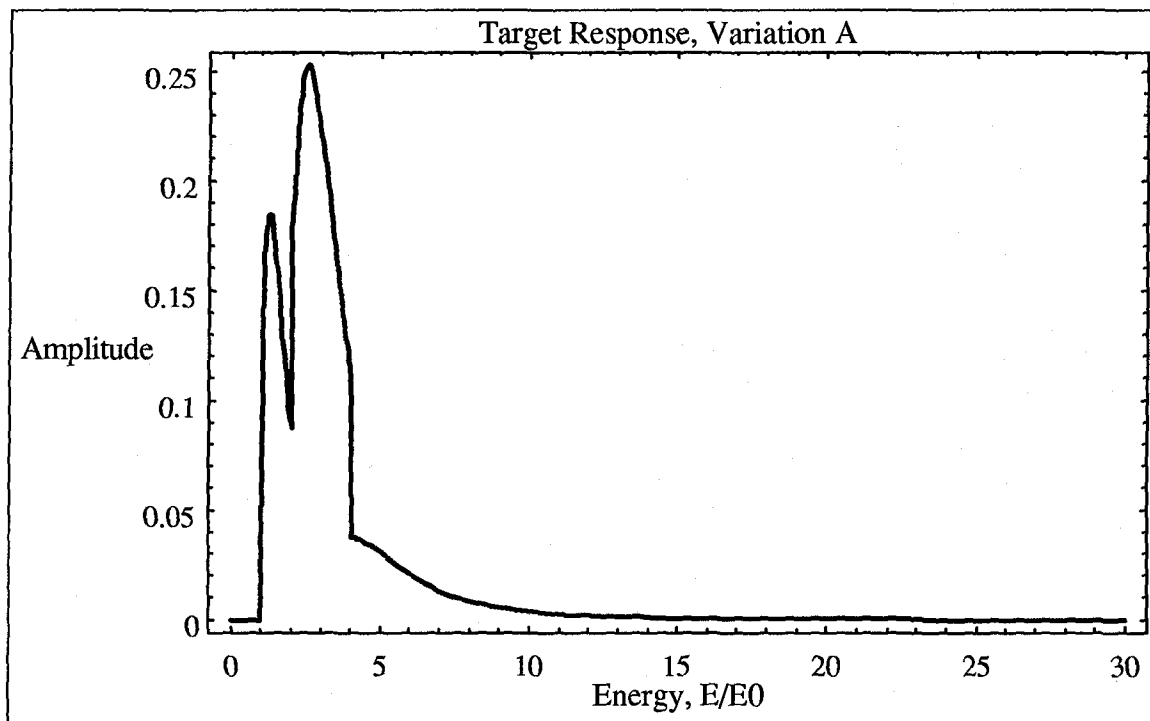


Figure 7. Test Target Response Function, Variation A

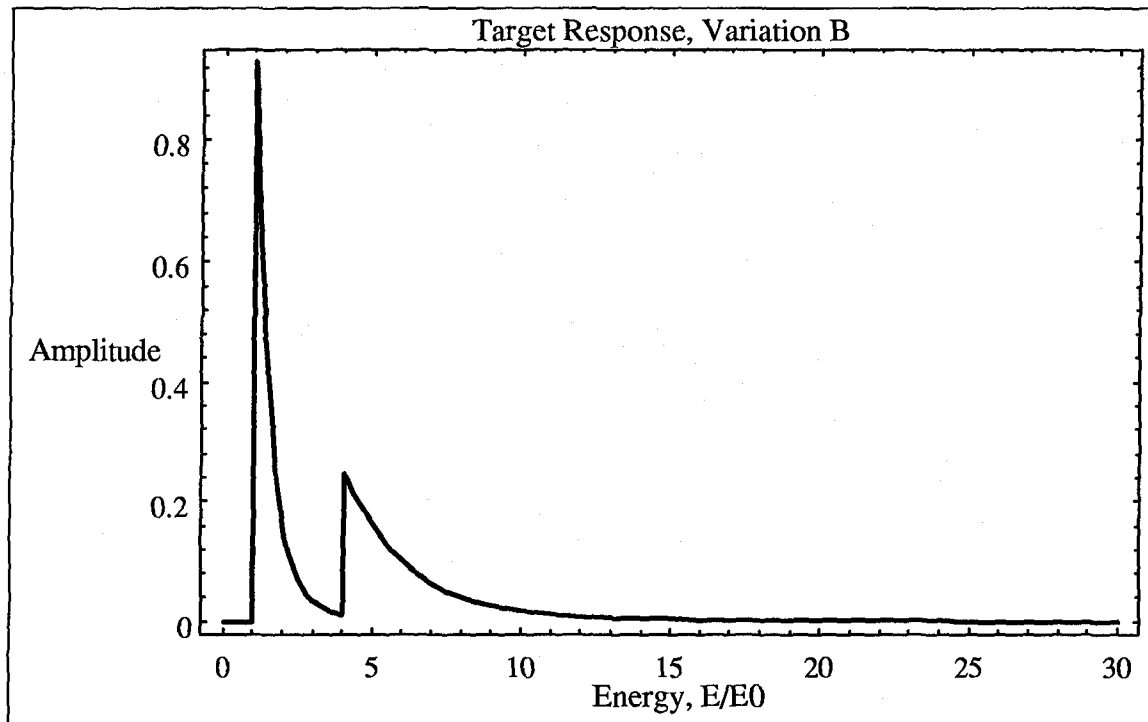


Figure 8. Test Target Response Function, Variation B

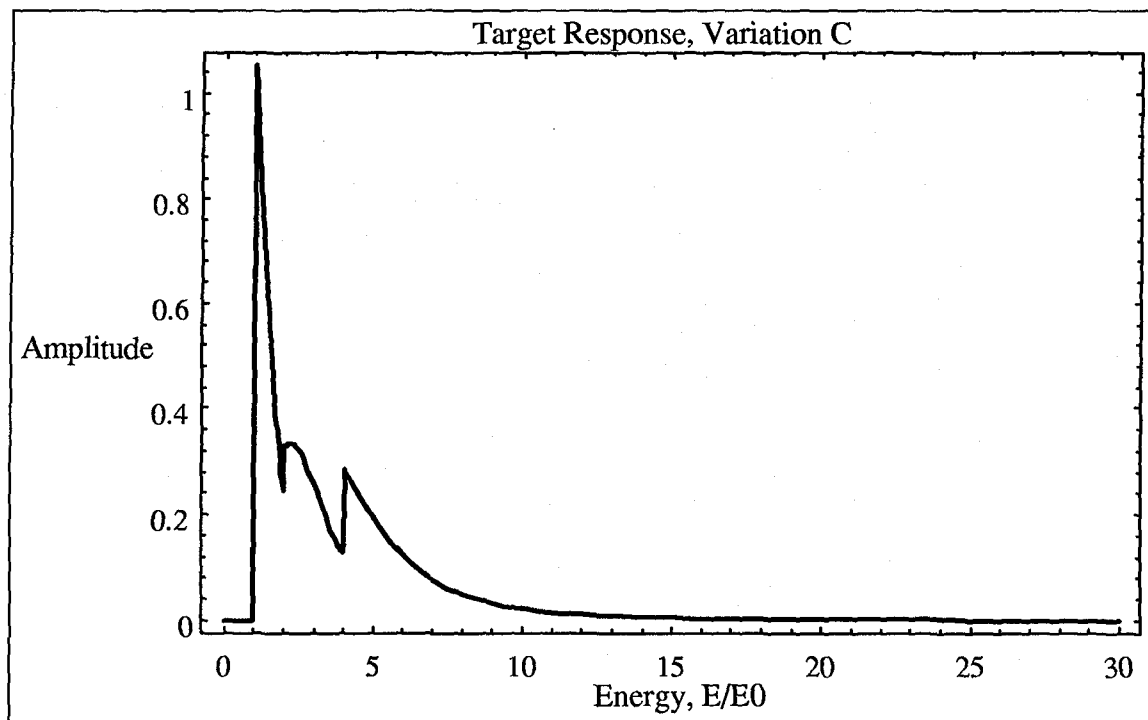


Figure 9. Test Target Response Function, Variation C

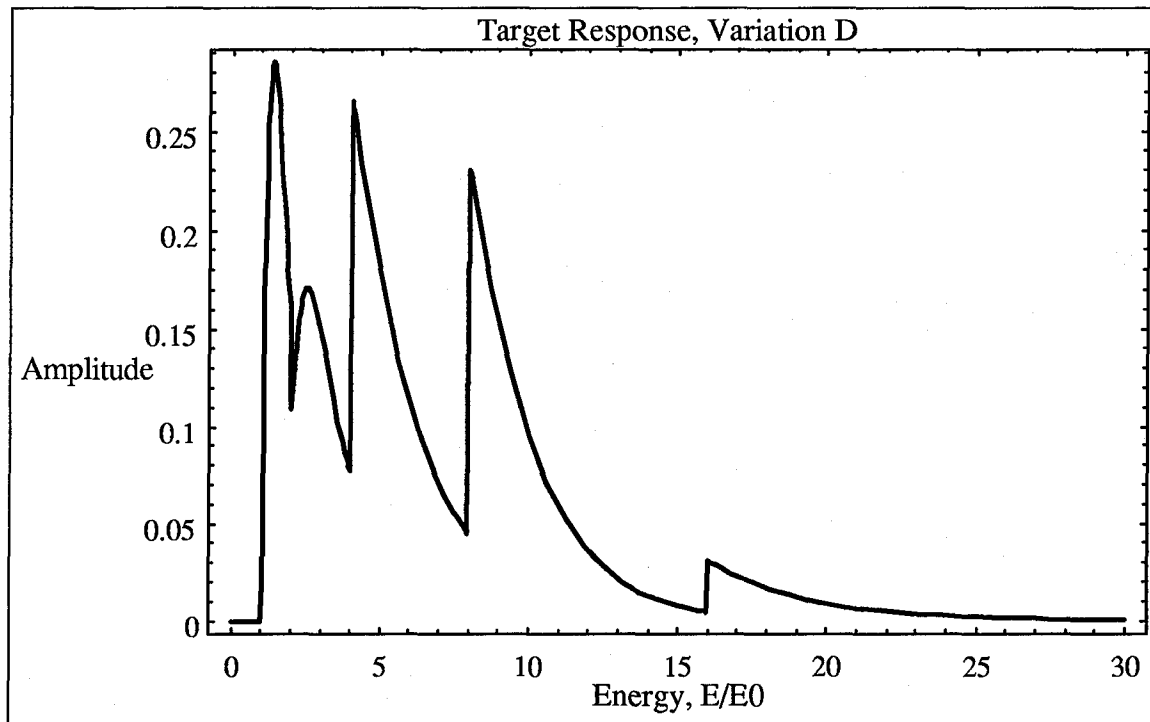


Figure 10. Test Target Response Function, Variation D

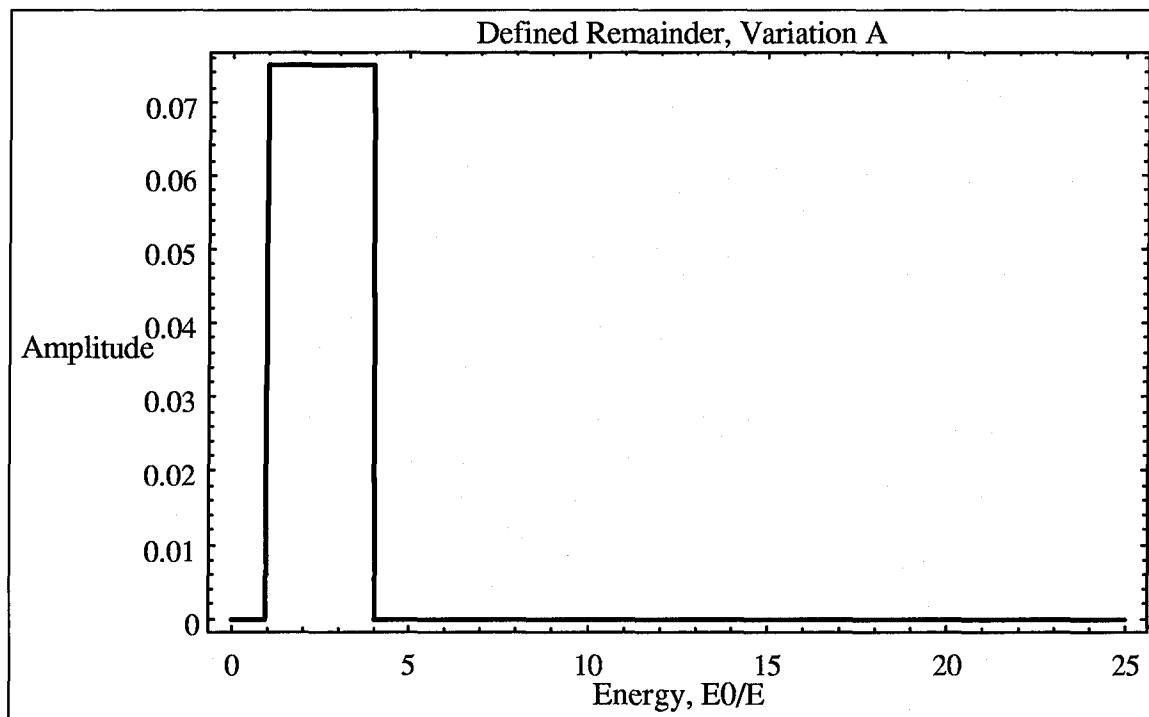


Figure 11. Defined Test  $T_{\bar{a}}(E)$ , Variation A

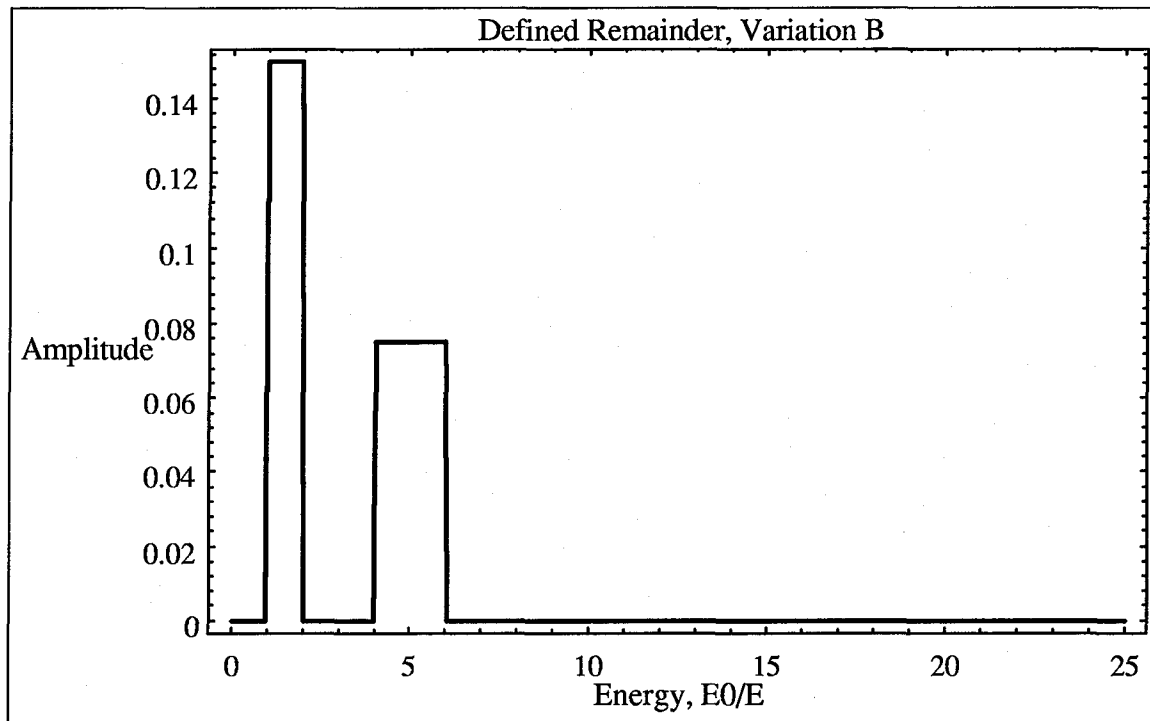


Figure 12. Defined Test  $T_{\bar{a}}(E)$ , Variation B

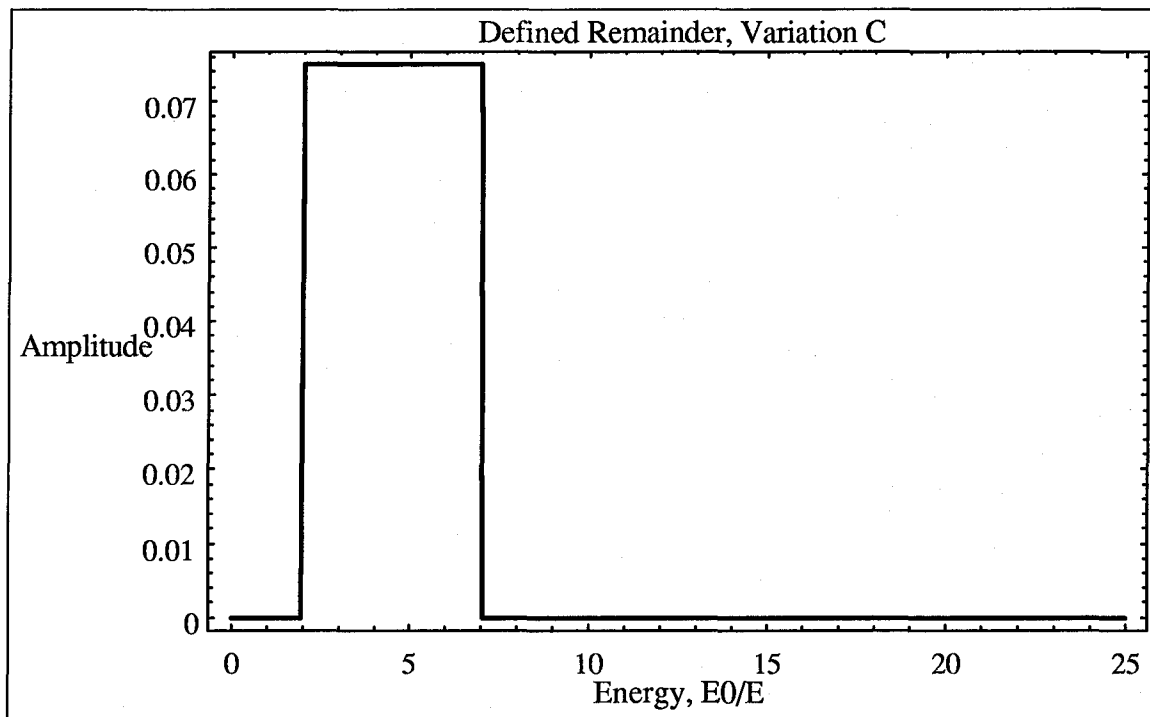


Figure 13. Defined Test  $T_{\bar{a}}(E)$ , Variation C

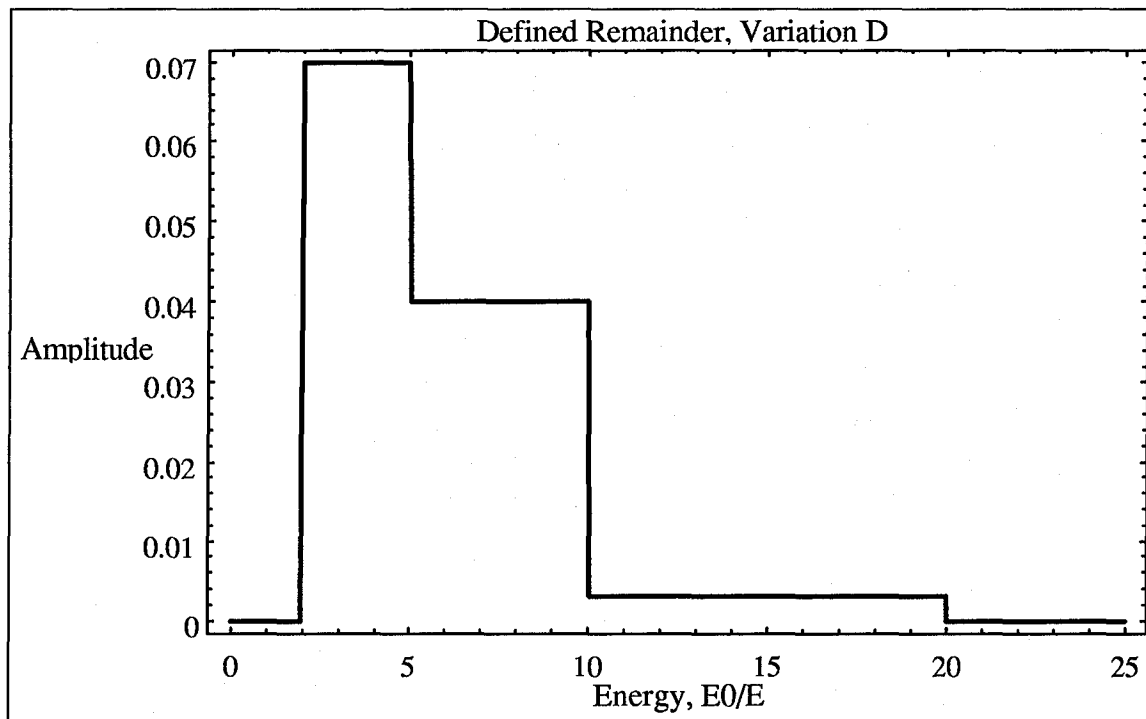


Figure 14. Defined Test  $T_{\bar{a}}(E)$ , Variation D

Examination of Figures 11-14 show that the  $T_{\bar{a}}(E)$  values are relatively small. This is due to the non-negativity constraint on  $T(E)$  (a concern when  $T_{\bar{a}}(E)$  is negative) and the fact that the  $T(E)$  responses shown in Figures 7-10 are relatively small in themselves.

Results of Test Case 1 (T1). T1.A defined the target response function as Eq (41a) with no correction term. The results of T1.A are summarized in Table 5.

Table 5 shows numerically calculated total target loading bounds of 30% for a target response function exactly defined as a positive combination of instrument responses. This supports the analytic argument from Chapter II that through-folding error simplifies to measurement error if  $T(E)$  is an exact combination of positive (or negative) terms. However, neither the upper nor lower defined bounds are found to be exactly 15%. The

difference between expected and calculated results are due to additional numeric error introduced via the numeric approximation of the instrument signal when  $a_i$  is not zero.

Optimization results are also shown in Table 5. Both maximum and minimum values were found via through-fold of closed detector system signals. This is expected as  $T(E)$  is defined using only closed system response functions. The optimization routines were unable to find the known minimum bound (30%); however, the total bound was reduced from 100% to 38.5%. The large optimized minimum bound (relative to maximum bound) is attributable to a relatively large negative value of  $a_5$  on error propagation. A complete discussion of error propagation is found in Bevington(1969:Ch 4).

Table 5. Test Results for Case T1.A

	$a_i$ , Naive Approach	Defined $a_i$	Optimized Max	Optimized Min
a1	0	1	0.1284	0.3427
a2	0	0	0.1778	1.1
a3	0	2.5	2.5494	1.3688
a4	0	0	0	1.0799
a5	0	0	0.0221	-0.9621
a6	0	0	0.0193	0.7827
a7	0	0	0.0158	0.5918
a8	0	0	-0.0026	0.821
a9	0	0	0	0
a10	0	0	0	0
a11	0	0	0	0
a12	0	0	0	0
$Z^U(a)$ , % +	50	13.5	17.1	n/a
$Z^U(a)$ , % -	50	16.5	n/a	21.4
Total Bound, %	100	30		38.5

T1.B proved to be a trivial variation on T1.A. The linear combination of open response functions from Eq (41b) was exactly reproduced by through-fold. The resulting total bound was found to be 30%. Again, a slight error due to signal computation was experienced. Results from T1.B are contained in Appendix C.

T1.C also proved to be trivial, despite the target response being defined as the exact linear combination of both open and closed response functions given by Eq (41c). All linear coefficients were of the same sign resulting in the total error bound being minimized to 30% using defined values for  $a_i$ . As found in validation, the upper and lower optimized bounds did not result from through-fold of the same type of detector systems. The overall optimized error bound was 35.1%--a slight improvement over the simpler model from T1.A. Results from T1.C are contained in Appendix C.

T1.D not only utilized both types of detector systems but defined  $T(E)$  as combinations of positive and negative terms (i.e., positive and negative  $a_i$ ) given by Eq (41d). The remainder term,  $T_{\bar{a}}(E)$ , remains defined as zero. The results of T1.D are summarized in Table 6. The influence of the negative coefficients on the error bound is significant for the defined selection of  $a_i$ . The total defined error bound increased from 30% to 91%. Because  $T_{\bar{a}}(E)$  is zero, the increase is attributable to numeric integration approximations of the signals and to propagation of errors associated with these signals due to the defined  $a_i$  (some being negative, other being positive).



Table 6. Test Results for Case T1.D

	$a_i$ , Naive Approach	Defined $a_i$	Optimized Max	Optimized Min
a1	0	4.2	0.829	0.762
a2	0	0	0.00002	1.3613
a3	0	1.5	1.6527	0.0002
a4	0	0	0	1.4865
a5	0	0	3.8724	-0.0002
a6	0	0	-1.7982	1.7565
a7	0	-3.5	4.7251	2.3024
a8	0	0	-5.3757	-1.7722
a9	0	-0.15	0	0
0	0			0
1	0			0
a12	0	2	0	0
$Z^U(a)$ , % +	50	48.6	12.2	n/a
$Z^U(a)$ , % -	50	42.8	n/a	22.6
Total Bound, %	100	91.4		34.8

Upper and lower optimized error bounds were both determined via through-fold of closed instrument signals. Total optimized bounds were less than 35%. This is consistent with values found in previous trials.

The importance of this variation is not only that through-fold can achieve tighter bounds than a defined set of  $a_i$  but that the optimal  $T_{\bar{a}}(E)$  is not always the minimum.

Figure 11 plots the value of  $T_{\bar{a}}(E)$  calculated from  $a_i$  for optimized upper bound.  $T_{\bar{a}}(E)$  was originally defined as zero. Figure 15 shows that the optimized  $T_{\bar{a}}(E)$  reflect the general characteristics (peaks and valleys) of the target response function (Figure 10).

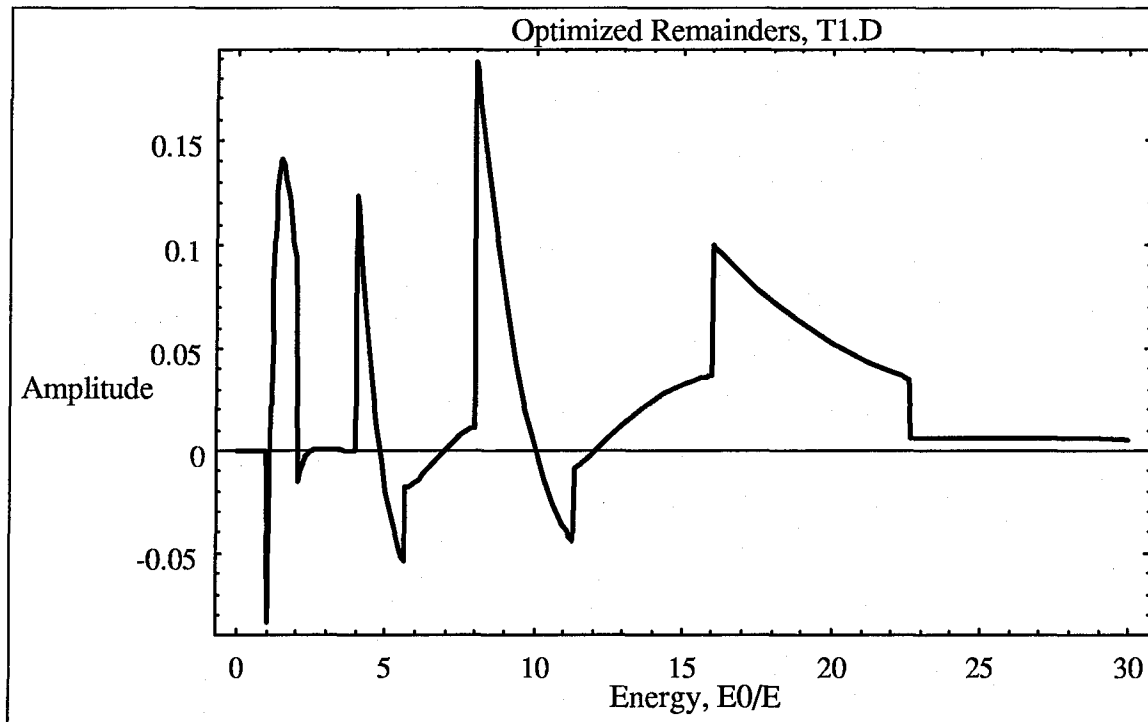


Figure 15. Optimized Remainder (Upper Bound),  $T_a(E)$ , for T1.D

Results of Test Case 2 (T2). The four variations of T2 were designed to investigate the effect on optimization when the defined target loading function includes a positive contribution from  $T_a(E)$ . Since the results of T2.A, T2.B, and T2.C were similar to each other, their results will only be briefly discussed. Results from T2.A, T2.B, and T2.C are contained in Appendix C.

The first three variations of T2 produced similar results. In all cases, naive error was verified to be  $\pm 50\%$ , the defined error increased from  $\pm 15\%$  (analytically and in T1) to  $\pm 24\%$ , and the optimized error bounds remained comparable to those of T1. Defined error increase is expected as  $T(E)$  is not an exact combination of instrument responses. The additional error is associated with propagation of the error associated with the non-

optimal  $T_{\bar{a}}(E)$  propagating into the exact spectrum (see explanation of Eq 22b). Unlike the results for the defined error bound, total optimized bounds remained constant with the addition of a remainder term to  $T(E)$ . Since the optimized bounds from T1 have the effects of error propagation included, large additional propagation errors are not expected in the optimized results of T2. Some additional error is expected with new selections over  $a_i$ ; however, the optimization of  $a_i$  minimizes additional error propagation.

Figure 16 compares T2.C's optimal  $T_{\bar{a}}(E)$  for the optimized upper bound to the defined  $T_{\bar{a}}(E)$ . Similar results were obtained for maximum and minimum bounds in T2.A, T2.B, and T2.C. Since all defined  $a_i$  were positive, the optimum  $T_{\bar{a}}(E)$  should be no larger than the defined  $T_{\bar{a}}(E)$ . Numeric integration from  $1E_1^0$  to  $40E_1^0$  of the curves in Figure 16 yield optimum  $T_{\bar{a}}(E) = 0.17$ , and defined  $T_{\bar{a}}(E) = 0.34$ .

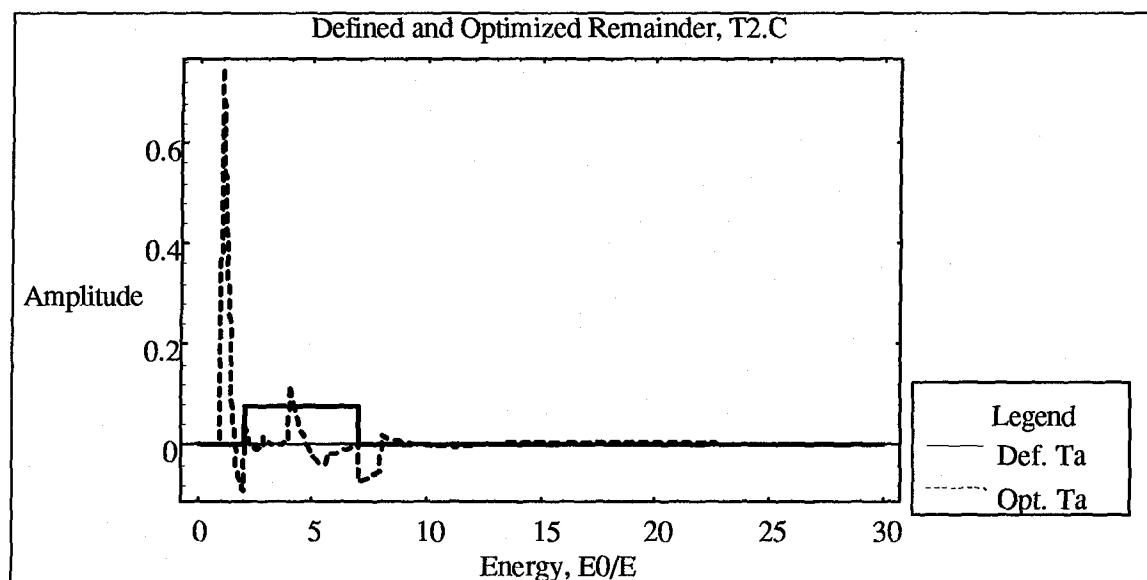


Figure 16. Case T2.C, Defined and Optimized (Upper Bound)  $T_{\bar{a}}(E)$

Test case T2.D used combinations of both types of detector response systems and allowed  $a_i$  to be combinations of positive and negative numbers. The remainder term was defined positive over all energies. T2.D results are presented in Table 7.

Table 7. Test Results for Case T2.D

	$a_i$ , Naive Approach	Defined $a_i$	Optimized Max	Optimized Min
a1	0	4.2	0.829	0.0734
a2	0	0	0.6938	1.4353
a3	0	1.5	1.606	0.454
a4	0	0	0.998	2.0913
a5	0	0	4.2905	0.0001
a6	0	0	1.2544	2.7684
a7	0	-3.5	4.1012	1.433
a8	0	-0.15	-4.614	-0.6655
a9	0	0	0	0
a10	0	0	0	0
a11	0	1	0	0
a12	0	2	0	0
$Z^U(a)$ , % +	50	42.1	13.3	n/a
$Z^U(a)$ , % -	50	37.8	n/a	21.9
Total Bound, %	100	79.9		35.2

As seen in test case T1.D, upon introduction of negative coefficients in the definition of the  $T(E)$ , the defined relative error bound more than doubled that of the cases having  $T_{\tilde{a}}(E) = 0$ . Optimized upper error bound has remained at 35%. Figure 17 plots the defined and optimized (upper bound)  $T_{\tilde{a}}(E)$  for case T2.D.

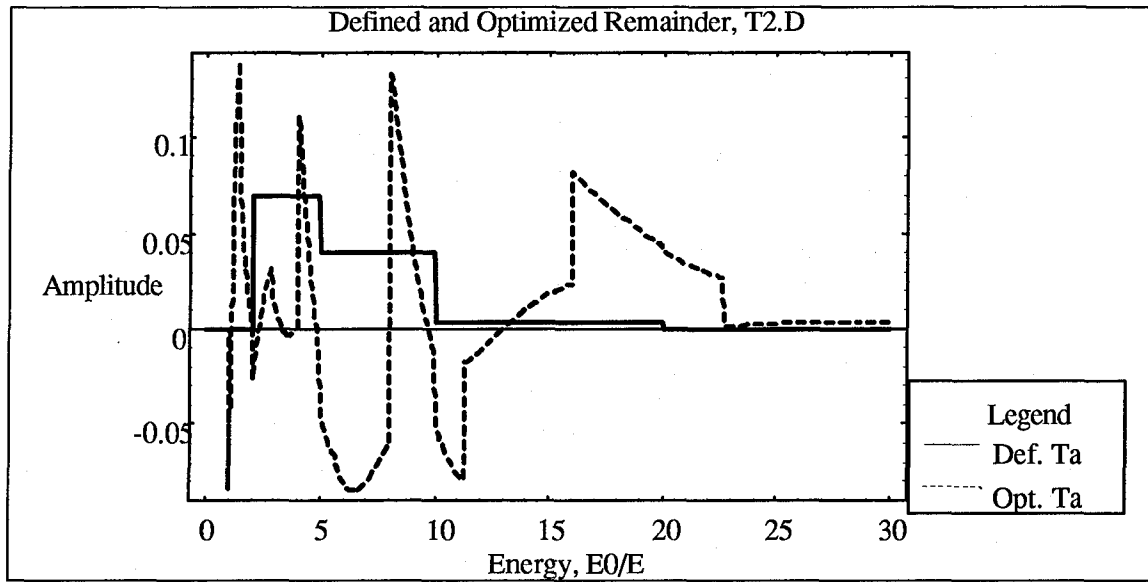


Figure 17. Case T2.D, Defined and Optimized (Upper Bound)  $T_{\bar{a}}(E)$

As with T1.D, the optimized  $T_{\bar{a}}(E)$  has no similarities to the defined  $T_{\bar{a}}(E)$ . However, the shape of T2D's optimized  $T_{\bar{a}}(E)$  is the same as in T1.D; small variations are expected (compared to T1D) because  $T(E)$  has changed by a small amount,  $T_{\bar{a}}(E)$ .

Results of Test Case 3 (T3). Test case three consisted of the same linear combinations of instrument responses as in T1 and T2 except a negative  $T_{\bar{a}}(E)$  was included. For consistency, the same  $T_{\bar{a}}(E)$  defined for cases T2 were used, however, they were subtracted from Eqs (41) instead of being added. The results from test case T3 parallel those of T2. The only notable differences are that defined and optimized bounds increased. The results of the trivial cases (T3.A, T3.B, and T3.C) are contained in Appendix C and are briefly discussed below.

In all cases, naive error was verified to be  $\pm 50\%$ , the defined error increased from  $\pm 24\%$  in T2 to  $\pm 50\%$  in T3, and the optimized error bounds increased from  $\pm 17\%$  in T2 to  $\pm 21\%$  in T3. The increase in defined error bound is again expected due to the negative contribution of  $T_{\bar{a}}(E)$ , in effect, mimicking a large negative  $a_i$ .

Figure 18 plots the defined and optimized (upper bound) remainders for T3.C. Similar results were obtained for upper and lower bounds in T3.A and T3.B. In the optimizer's attempt to represent the complete target response as a set of linear terms, the total area under the optimized  $T_{\bar{a}}(E)$  curve in Figure 18 was driven negative. The results from the overall negative  $T_{\bar{a}}(E)$  on error propagation are akin to selection of additional negative  $a_i$  values. Hence the error bounds associated with an overall negative  $T_{\bar{a}}(E)$  are expected to increase over other cases.

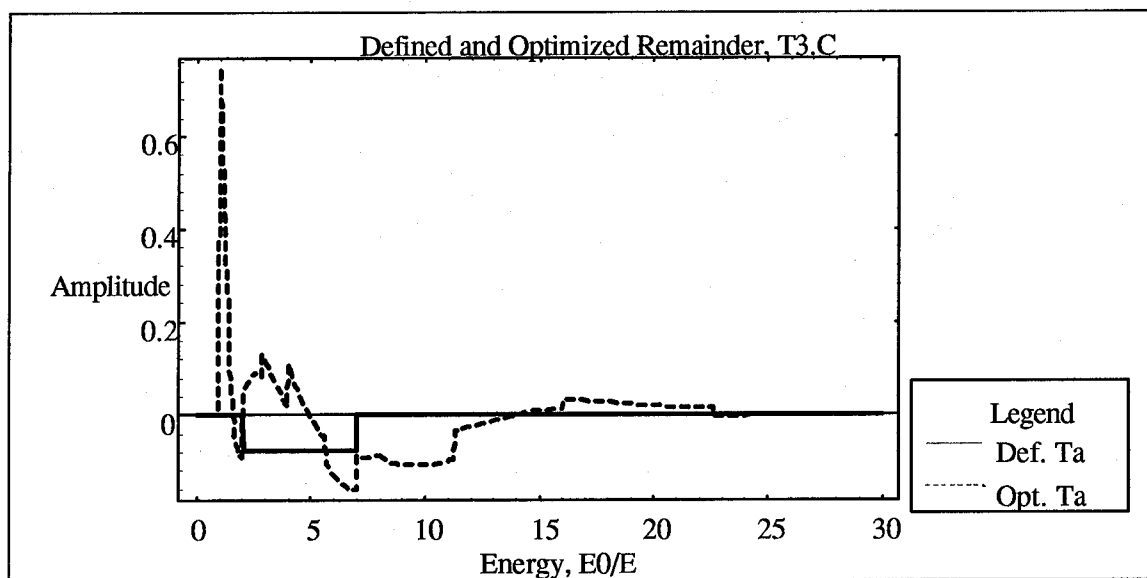


Figure 18. Case T3.C, Defined and Optimized (Upper Bound)  $T_{\bar{a}}(E)$

The results from T3.D are shown in Table 8. The overall influence of  $T(E)$  being explicitly defined with a negative correction term is an increase in through-fold bounds to 47%. However, the bounds are still a considerable improvement over the naive approach.

Table 8. Test Results for Case T3.D

	$a_i$ , Naive Approach	Defined $a_i$	Optimized Max	Optimized Min
a1	0	4.2	0.8284	0
a2	0	0	0.5878	0
a3	0	1.5	0.0871	0
a4	0	0	0	0
a5	0	0	2.6229	0
a6	0	0	-1.4672	0
a7	0	-3.5	4.679	0
a8	0	0	-5.2097	0
a9	0	-0.3	0	0.1583
a10	0	0	0	0.193
a11	0	1	0	0.6819
a12	0	2	0	1.238
$Z^U(a)$ , % +	50	99.8	19.1	n/a
$Z^U(a)$ , % -	50	90.1	n/a	27.5
Total Bound, %	100	189.9		46.6

## V. Summary and Conclusions

### Summary

Validation of Method. The purpose of the validation case is to ensure that the through-fold routine is operating properly. The validation case was set up with two goals: 1) verifying through-folds capabilities to simulate the case of having no experiment and 2) verification that target loading bounds can be decreased from the no experiment case. Through-fold proved capable of predicting pre-test error bounds and of utilizing test data to reduce the pre-test prediction.

Test Cases. The overall goal of the test cases was to explore the feasibility of through-fold. A series of test cases was set up to compare the through-fold results to the expectations for the method. The test cases were set up to incrementally increase the complexity of a problem. Test case one assumed target loading was a linear combination of instrument responses. Test case two, increased the complexity of the problem by assuming there was a positive remainder term. Finally, test case three allowed the remainder to be negative. To aid in evaluation, each test case consisted of four separate combinations of detection system signals.

All basic expectations for the through-fold were met. Results from test case one indicated that through-fold could predict reasonable bounds on an unknown function. Results from case two demonstrated the anticipated behavior concerning error propagation. The results from the more complicated problem presented in test case three



showed a reduction in predicted error bounds from the naive case and from the error bound based on the defined values for the target loading response functions.

### Conclusions

The results from the validation and test cases support the following conclusions:

1. Through-fold consistently reduced the error bounds associated with the test cases. However, the combination of energy bin resolution and small spectrum and target loading values in some of the bins may have limited the capabilities of the through-fold routine.
2. Optimization of error bounds has a limiting factor dependent on propagation of errors and the actual spectrum and response functions used.
3. The optimization does not always occur when the target response function is defined exactly.
4. Although there is some degree of user judgment involved in selection of the starting values for the optimization routines, the resulting target loading bounds did not appear to be sensitive to the selection.
5. The simplified target loading problem was adequately handled by through-fold.

The results of test cases two and three (where through-fold consistently outperformed results calculated from exact target response functions) indicate promise for the technique.

## VI. Recommendations

The following are recommendations for continued work in this area. First, a more robust optimization routine must be found. This could solve a few of the problems experienced. A different optimization routine may speed up calculations, should be capable of finding exact solutions for problems used in test case one, and should be capable of handling the quadratic problem which was simplified to a linear one for this study. It is hoped that insight gained into the through-fold methodology from the linear programming problem will carry over to quadratic programming problem. Second, different choices of input data should be used to verify that through-fold results are similar in more realistic test cases. Finally, a third area of study must consider how well through-fold agrees with output from accepted unfolding routines.

## Appendix A: Formal Derivation of Through-Fold Equations

### Definition of Terms

$\sim$	=	tilde, denotes an exact quantity, as opposed to measured
$\delta$	=	delta, denotes correction term determined from measurement error, calibration error, or a conservative estimate
$R_i(E)$	=	instrument response as a function of energy, $i^{\text{th}}$ instrument
$S(E)$	=	spectrum as a function of energy
$T(E)$	=	target response as a function of energy
$Y_i$	=	instrument signal, $i^{\text{th}}$ instrument
$Z$	=	target loading

NOTE: The absence of both tilde and delta indicates the quantity is measured or calibrated.

The derivation begins with a definition of target loading. Target loading can be viewed as the signal which would have been recorded by the target had it actually been an error free instrument. Target loading can be represented similarly to instrument signal by:

$$\tilde{Z} = \int_0^{\infty} \tilde{S}(E) \tilde{T}(E) dE \quad (\text{A1})$$

None of the values in Eq (A1) are actually known. They can, however, be approximated by a measured or predicted value plus a correction term. If the predicted target response

is further approximated as a linear combination of the instrument responses plus a remainder, to keep the relationship exact, then all the terms on the right hand side of Eq (A1) can be replaced with known predicted, or boundable values. Defining the terms:

$$\tilde{S}(E) = S(E) + \delta S(E) \quad (\text{A2.a})$$

$$\tilde{T}(E) = T(E) + \delta T(E) \quad (\text{A2.b})$$

$$\tilde{R}_i(E) = R_i(E) + \delta R_i(E) \quad (\text{A2.c})$$

$$\tilde{Y}_i = Y_i + \delta Y_i \quad (\text{A2.d})$$

Equations (A2) should be read as 'the exact value equals the measured value plus a correction term'. The four correction terms in Eqs (A2) are based on a conservative estimates (the first two), calibration error, and measurement error respectively.

#### Derivation

Since all terms on the right hand sides (RHS) of Eqs (A2) are considered known, they can be substituted into the exact target loading equation, eliminating the unknowns. Substituting Eq (A2.b) into Eq (A1) yields:

$$\tilde{Z} = \int_0^{\infty} \tilde{S}(E) [T(E) + \delta T(E)] dE \quad (\text{A3})$$

Now let

$$\tilde{Z} = Z + \delta Z \quad (\text{A4})$$

where,

$$Z = \int_0^{\infty} \tilde{S}(E) T(E) dE \quad (\text{A4.a})$$

$$\delta Z = \int_0^{\infty} \tilde{S}(E) \delta T(E) dE \quad (\text{A4.b})$$

Assuming  $T(E)$  can be approximated by a linear combination of instrument response functions plus a correction term (remainder), yields the following approximation:

$$T(E) = \sum_i a_i R_i(E) + T_{\bar{a}}(E) \quad (\text{A5})$$

where

$a_i$  = a constant for the  $i^{\text{th}}$  instrument

$T_{\bar{a}}(E)$  = a remainder based on the choice of  $a_i$

Substituting this last equation into Eq (A4.a),

$$Z = \int_0^{\infty} \tilde{S}(E) \left[ \sum_i a_i R_i(E) + T_{\bar{a}}(E) \right] dE \quad (\text{A6})$$

or, by expanding the integral and reversing the order of integration and summation:

$$Z = \sum_i a_i \int_0^{\infty} \tilde{S}(E) R_i(E) dE + \int_0^{\infty} \tilde{S}(E) T_{\bar{a}}(E) dE \quad (\text{A7})$$

The exact spectrum in Eq (A7) can now be replaced with its approximation from Eq

(A2.a). However instead of replacing  $\tilde{S}(E)$  in both integrals, it is beneficial to replace

$R_i(E)$  in the first integral of Eq (A7) with its value from Eq (A2.c) and then to substitute the approximation of the exact spectrum into the second part of Eq (A7). This trick yields:

$$\begin{aligned}
 Z = & \sum_i a_i \int_0^{\infty} \tilde{S}(E) \tilde{R}_i(E) dE - \sum_i a_i \int_0^{\infty} \tilde{S}(E) \delta R_i(E) dE \\
 & + \int_0^{\infty} S(E) T_{\tilde{a}}(E) dE + \int_0^{\infty} \delta S(E) T_{\tilde{a}}(E) dE
 \end{aligned} \tag{A8}$$

The above trick has introduced the exact signal, the first integral of Eq (A8), into our equation. We will now introduce data (measured signals) into our problem by approximating of the exact signal using Eq (A2.d).

$$\begin{aligned}
 Z = & \sum_i a_i Y_i + \sum_i a_i \delta Y_i - \sum_i a_i \int_0^{\infty} \tilde{S}(E) \delta R_i(E) dE \\
 & + \int_0^{\infty} S(E) T_{\tilde{a}}(E) dE + \int_0^{\infty} \delta S(E) T_{\tilde{a}}(E) dE
 \end{aligned} \tag{A9}$$

Substituting the approximation of the exact spectrum for  $\tilde{S}(E)$ .

$$\begin{aligned}
 Z = & \sum_i a_i Y_i + \sum_i a_i \delta Y_i \\
 & - \sum_i a_i \int_0^{\infty} S(E) \delta R_i(E) dE - \sum_i a_i \int_0^{\infty} \delta S(E) \delta R_i(E) dE \\
 & + \int_0^{\infty} S(E) T_{\tilde{a}}(E) dE + \int_0^{\infty} \delta S(E) T_{\tilde{a}}(E) dE
 \end{aligned} \tag{A10}$$

Now that all the exact terms have been eliminated from  $Z$ , we can switch our attention to the  $\delta Z$  term from Eq (A4.b). For this term all we have to do is substitute the approximation of the exact spectrum and simplify it to:

$$\delta z = \int_0^{\infty} S(E) \delta T(E) dE + \int_0^{\infty} \delta S(E) \delta T(E) dE \quad (A11)$$

Finally, we can combine equations (A10) and (A11) for the exact target loading:

$$\begin{aligned} \tilde{Z} = & \sum_i a_i Y_i + \sum_i a_i \delta Y_i \\ & - \sum_i a_i \int_0^{\infty} S(E) \delta R_i(E) dE - \sum_i a_i \int_0^{\infty} \delta S(E) \delta R_i(E) dE \\ & + \int_0^{\infty} S(E) T_{\bar{a}}(E) dE + \int_0^{\infty} \delta S(E) T_{\bar{a}}(E) dE \\ & + \int_0^{\infty} S(E) \delta T(E) dE + \int_0^{\infty} \delta S(E) \delta T(E) dE \end{aligned} \quad (A12)$$

The final equation for target loading is found by writing the above equation explicitly in terms of the constants,  $a_i$ , by replicating  $T_{\bar{a}}(E)$  with its value from Eq (A5):

$$\begin{aligned}
\tilde{Z} = & \sum_i a_i Y_i + \sum_i a_i \delta Y_i \\
& - \sum_i a_i \int_0^\infty S(E) \delta R_i(E) dE - \sum_i a_i \int_0^\infty \delta S(E) \delta R_i(E) dE \\
& + \int_0^\infty S(E) \left[ T(E) - \sum_j a_j R_j(E) \right] dE + \int_0^\infty \delta S(E) \left[ T(E) - \sum_j a_j R_j(E) \right] dE \\
& + \int_0^\infty S(E) \delta T(E) dE + \int_0^\infty \delta S(E) \delta T(E) dE
\end{aligned} \tag{A13}$$

Expanding the two integrals that were changed,

$$\begin{aligned}
\tilde{Z} = & \sum_i a_i Y_i + \sum_i a_i \delta Y_i \\
& - \sum_i a_i \int_0^\infty S(E) \delta R_i(E) dE - \sum_i a_i \int_0^\infty \delta S(E) \delta R_i(E) dE \\
& + \int_0^\infty S(E) T(E) dE - \int_0^\infty S(E) \sum_j a_j R_j(E) dE \\
& + \int_0^\infty \delta S(E) T(E) dE - \int_0^\infty \delta S(E) \sum_j a_j R_j(E) dE \\
& + \int_0^\infty S(E) \delta T(E) dE + \int_0^\infty \delta S(E) \delta T(E) dE
\end{aligned} \tag{A14}$$

Reordering the terms, to include reversing the order of integration and summation:



$$\begin{aligned}
\tilde{Z} = & \sum_i a_i Y_i + \sum_i a_i \delta Y_i \\
& - \sum_i a_i \int_0^{\infty} S(E) R_i(E) dE - \sum_i a_i \int_0^{\infty} \delta S(E) R_i(E) dE \\
& - \sum_i a_i \int_0^{\infty} S(E) \delta R_i(E) dE - \sum_i a_i \int_0^{\infty} \delta S(E) \delta R_i(E) dE \quad (A15) \\
& + \int_0^{\infty} S(E) T(E) dE + \int_0^{\infty} \delta S(E) T(E) dE \\
& + \int_0^{\infty} S(E) \delta T(E) dE + \int_0^{\infty} \delta S(E) \delta T(E) dE
\end{aligned}$$

Now that we have an expression for the target loading, and bounds on all the delta terms, we need to convert the analytic expression to a numeric one.

#### Conversion to a Numeric Solution

There are two forms of integrals in Eq (A15) which need conversion to numeric techniques, those with the instrument response function involved and those with the target response function involved. Both integrals can be numerically approximated using a summation over the energy range of concern. Using this form of approximation, basic instrument signal and target response integrals can be written as:

$$y_i = \sum_{j=1}^N S(E_j) R_i(E_j) \Delta E_j \quad (A16.a)$$

and

$$z = \sum_{j=1}^N S(E_j) T(E_j) \Delta E_j \quad (\text{A16.b})$$

where

$y_i$  = a basic approximation to signal recorded by the  $i^{\text{th}}$  instrument

$S(E_j)$  = the predicted spectrum at energy step  $j$

$R_i(E_j)$  = the response function of the  $i^{\text{th}}$  instrument (as measured)

$\Delta E_j$  = the width of the  $j^{\text{th}}$  energy step

$z$  = a basic approximation to target signal

$T(E_j)$  = the predicted target response at energy step  $j$

$N$  = the number of energy groups

Replacing the integrals in Eq (A15) with summations yields:

$$\begin{aligned} \tilde{Z} = & \sum_i a_i Y_i + \sum_i a_i \delta Y_i \\ & - \sum_i a_i \sum_{j=1}^N S(E_j) R_i(E_j) \Delta E_j - \sum_i a_i \sum_{j=1}^N \delta S(E_j) R_i(E_j) \Delta E_j \\ & - \sum_i a_i \sum_{j=1}^N S(E_j) \delta R_i(E_j) \Delta E_j - \sum_i a_i \sum_{j=1}^N \delta S(E_j) \delta R_i(E_j) \Delta E_j \quad (\text{A17}) \\ & + \sum_{j=1}^N S(E_j) T(E_j) \Delta E_j + \sum_{j=1}^N \delta S(E_j) T(E_j) \Delta E_j \\ & + \sum_{j=1}^N S(E_j) \delta T(E_j) \Delta E_j + \sum_{j=1}^N \delta S(E_j) \delta T(E_j) \Delta E_j \end{aligned}$$

To make the above calculation easier, it is beneficial to form an instrument response matrix,  $\mathbf{R}$ , a spectrum vector,  $\mathbf{s}$ , and a target response vector,  $\mathbf{t}$ , of the predicted functions.

$$\begin{aligned}(\mathbf{R})_{ij} &= R_i(E_j) \Delta E_j \\(\mathbf{s})_j &= S(E_j) \\(\mathbf{t})_j &= T(E_j) \Delta E_j\end{aligned}\tag{A18}$$

Equations (A16 ) can now be converted to vector notation, given by

$$\sum_{j=1}^N S(E_j) R_i(E_j) \Delta E_j = \mathbf{R} \cdot \mathbf{s}$$

and

(A19)

$$\sum_{j=1}^N S(E_j) T(E_j) \Delta E_j = \mathbf{s} \cdot \mathbf{t}$$

Utilizing the vector notation from Eq (A18) to represent the summations:

$$\begin{aligned}\tilde{Z} &= \sum_i a_i Y_i + \sum_i a_i \delta Y_i \\&- \sum_i a_i \mathbf{R} \cdot \mathbf{s} - \sum_i a_i \mathbf{R} \cdot \delta \mathbf{s} \\&- \sum_i a_i \delta \mathbf{R} \cdot \mathbf{s} - \sum_i a_i \delta \mathbf{R} \cdot \delta \mathbf{s} \\&+ \mathbf{s} \cdot \mathbf{t} + \delta \mathbf{s} \cdot \mathbf{t} \\&+ \mathbf{s} \cdot \delta \mathbf{t} + \delta \mathbf{s} \cdot \delta \mathbf{t}\end{aligned}\tag{A20}$$

Realizing that the instrument signals can be represented by the vector  $(y)_i = [Y_i]$  and that the  $a_i$  can be represented by a similar vector equation, allows the previous equation to be written completely in terms of vectors and matrixes:

$$\begin{aligned}
 \tilde{Z} = & \mathbf{a} \cdot \mathbf{y} + \mathbf{a} \cdot \delta \mathbf{y} \\
 & - \mathbf{a} \cdot \mathbf{R} \cdot \mathbf{s} - \mathbf{a} \cdot \mathbf{R} \cdot \delta \mathbf{s} \\
 & - \mathbf{a} \cdot \delta \mathbf{R} \cdot \mathbf{s} - \mathbf{a} \cdot \delta \mathbf{R} \cdot \delta \mathbf{s} \\
 & + \mathbf{s} \cdot \mathbf{t} + \delta \mathbf{s} \cdot \mathbf{t} \\
 & + \mathbf{s} \cdot \delta \mathbf{t} + \delta \mathbf{s} \cdot \delta \mathbf{t}
 \end{aligned} \tag{A21}$$

Making use of the distributive property of dot products simplifies the exact target loading equation becomes:

$$\begin{aligned}
 \tilde{Z} = & \mathbf{a} \cdot (\mathbf{y} + \delta \mathbf{y} - \mathbf{R} \cdot \mathbf{s} - \mathbf{R} \cdot \delta \mathbf{s} - \delta \mathbf{R} \cdot \mathbf{s} - \delta \mathbf{R} \cdot \delta \mathbf{s}) \\
 & + \mathbf{s} \cdot \mathbf{t} + \delta \mathbf{s} \cdot \mathbf{t} + \mathbf{s} \cdot \delta \mathbf{t} + \delta \mathbf{s} \cdot \delta \mathbf{t}
 \end{aligned} \tag{A22}$$

Equation (A22) is an exact expression for target loading because the exact correction vectors,  $\delta \mathbf{s}$ ,  $\delta \mathbf{y}$ ,  $\delta \mathbf{R}$ , and  $\delta \mathbf{t}$  have been carried throughout the derivation. Unfortunately, Eq (A22) can not be computed because the exact delta values are unknown.

Bounds on Exact Target Loading. The value of  $\tilde{Z}$  given by Eq (A22) cannot be calculated because the delta terms are not known exactly, only within the bounds on the correction terms discussed previously. The exact target loading can be bound by

$$Z^L \leq \tilde{Z} \leq Z^U \tag{A23}$$

where  $Z^U$  and  $Z^L$  are the upper and lower bounds respectively on target loading.

The upper (lower) target loading bounds defined above can be computed for any fixed choice of  $\mathbf{a}$  by choosing the values for  $\delta\mathbf{s}$ ,  $\delta\mathbf{y}$ ,  $\delta\mathbf{R}$ , and  $\delta\mathbf{t}$  -- all being allowed to vary (within the error bounds) at each energy bin -- to maximize (minimize) the target loading expression, which is implicitly a function of  $\mathbf{a}$ . These bounds are computed by solving the following linear programs for the upper and lower target loading bounds respectively:

$$Z^U(\mathbf{a}) = \text{Max}_{\delta\mathbf{y}, \delta\mathbf{s}, \delta\mathbf{R}, \delta\mathbf{t}} \left[ \mathbf{a} \cdot \left( \mathbf{y} + \delta\mathbf{y} - \mathbf{R} \cdot \mathbf{s} - \mathbf{R} \cdot \delta\mathbf{s} - \delta\mathbf{R} \cdot \mathbf{s} - \delta\mathbf{R} \cdot \delta\mathbf{s} \right) + \mathbf{s} \cdot \mathbf{t} + \delta\mathbf{s} \cdot \mathbf{t} + \mathbf{s} \cdot \delta\mathbf{t} + \delta\mathbf{s} \cdot \delta\mathbf{t} \right] \quad (\text{A24})$$

$$Z^L(\mathbf{a}) = \text{Min}_{\delta\mathbf{y}, \delta\mathbf{s}, \delta\mathbf{R}, \delta\mathbf{t}} \left[ \mathbf{a} \cdot \left( \mathbf{y} + \delta\mathbf{y} - \mathbf{R} \cdot \mathbf{s} - \mathbf{R} \cdot \delta\mathbf{s} - \delta\mathbf{R} \cdot \mathbf{s} - \delta\mathbf{R} \cdot \delta\mathbf{s} \right) + \mathbf{s} \cdot \mathbf{t} + \delta\mathbf{s} \cdot \mathbf{t} + \mathbf{s} \cdot \delta\mathbf{t} + \delta\mathbf{s} \cdot \delta\mathbf{t} \right]$$

In Eq (A24)  $\delta\mathbf{s}$ ,  $\delta\mathbf{y}$ ,  $\delta\mathbf{R}$ , and  $\delta\mathbf{t}$  are the variables subject to the following constraints:

$$\delta\mathbf{y}_{\min} \leq \delta\mathbf{y} \leq \delta\mathbf{y}_{\max}$$

$$\delta\mathbf{s}_{\min} \leq \delta\mathbf{s} \leq \delta\mathbf{s}_{\max}$$

$$\delta\mathbf{R}_{\min} \leq \delta\mathbf{R} \leq \delta\mathbf{R}_{\max}$$

$$\delta\mathbf{t}_{\min} \leq \delta\mathbf{t} \leq \delta\mathbf{t}_{\max}$$

(A25)

$\mathbf{R}$ ,  $\mathbf{s}$ ,  $\mathbf{t}$ , and  $\mathbf{y}$  are input data; and  $\mathbf{a}$  is the variable for which the bound is to be determined.

The goal functions of both bounds in Eq (A24) are the same and are given by:

$$\begin{aligned}
f(\delta y, \delta s, \delta R, \delta t) = & \mathbf{a} \cdot (\mathbf{y} + \delta \mathbf{y} - \mathbf{R} \cdot \mathbf{s} - \mathbf{R} \cdot \delta \mathbf{s} - \delta \mathbf{R} \cdot \mathbf{s} - \delta \mathbf{R} \cdot \delta \mathbf{s}) \\
& + \mathbf{s} \cdot \mathbf{t} + \delta \mathbf{s} \cdot \mathbf{t} + \mathbf{s} \cdot \delta \mathbf{t} + \delta \mathbf{s} \cdot \delta \mathbf{t}
\end{aligned} \tag{A26}$$

The upper bound is found by maximum the goal function over the  $\delta \mathbf{s}$ ,  $\delta \mathbf{y}$ ,  $\delta \mathbf{R}$ , and  $\delta \mathbf{t}$ .

Similarly, the lower bound is found by minimizing the goal function over the  $\delta \mathbf{s}$ ,  $\delta \mathbf{y}$ ,  $\delta \mathbf{R}$ , and  $\delta \mathbf{t}$ . The resulting values for  $Z^U(\mathbf{a})$  and  $Z^L(\mathbf{a})$  from Eq (A24) represent the largest possible bounds (maximum and minimum respectively) on target loading for fixed set of  $\mathbf{a}$ . However, it should be possible to tighten these bounds by selecting appropriate sets of  $\mathbf{a}$ . The process of selecting the  $\mathbf{a}$ 's resulting in the tightest possible bounds is accomplished by optimizing the upper and lower bound over all possible choices of  $\mathbf{a}$ . The result is a classic minimum-maximum (mini-max) problem given by:

$$\begin{aligned}
Z_{\min}^U &= \underset{\mathbf{a}}{\text{Min}} [Z^U(\mathbf{a})] \\
Z_{\max}^L &= \underset{\mathbf{a}}{\text{Max}} [Z^L(\mathbf{a})]
\end{aligned} \tag{A27}$$

$Z_{\min}^U$  is the minimum upper bound (least upper bound) for target loading and is found by minimizing  $Z^U(\mathbf{a})$  over  $\mathbf{a}$ .  $Z_{\max}^L$  is the maximum lower bound for target loading, found by maximizing  $Z^L(\mathbf{a})$  over  $\mathbf{a}$ . The outer loop of the mini-max problem produces an unconstrained (the  $\mathbf{a}$  vector can take on any values) quadratic problem.

Standard Form. The goal function in Eq (A26) can not directly be used in a quadratic programming problem because it is not in standard form. The standard form for linear programming problems generally require non-negative variables. The bounded error terms are therefore defined as the difference of two positive numbers

$$\begin{aligned}
 \delta y &= \delta y^+ - \delta y^- \\
 \delta s &= \delta s^+ - \delta s^- \\
 \delta R &= \delta R^+ - \delta R^- \\
 \delta t &= \delta t^+ - \delta t^-
 \end{aligned} \tag{A28}$$

where all the terms on the RHS of Eq (A28) are greater than or equal to zero.

The inner loops of the mini-max problems will force one of the terms on the RHS of Eq (A28) to zero and the other to its maximum magnitude at each energy bin. The first term will be zero if the error is negative while the second term will be zero if the error is positive. Inserting the non-negativity constraints into the goal function, Eq (A26):

$$\begin{aligned}
 f(\delta y, \delta s, \delta R, \delta t) = a \cdot & \left\{ \begin{aligned} & y + (\delta y^+ - \delta y^-) - R \cdot s \\ & - R \cdot (\delta s^+ - \delta s^-) - (\delta R^+ - \delta R^-) \cdot s \\ & - [(\delta R^+ - \delta R^-) \cdot (\delta s^+ - \delta s^-)] \end{aligned} \right\} \\
 & + s \cdot t + (\delta s^+ - \delta s^-) \cdot t + s \cdot (\delta t^+ - \delta t^-) \\
 & + [(\delta s^+ - \delta s^-) \cdot (\delta t^+ - \delta t^-)]
 \end{aligned} \tag{A29}$$

or

$$f(\delta y, \delta s, \delta R, \delta t) = a \cdot \left\{ \begin{array}{l} y + \delta y^+ - \delta y^- - R \cdot s \\ - R \cdot \delta s^+ + R \cdot \delta s^- - \delta R^+ \cdot s + \delta R^- \cdot s \\ - \left[ \delta R^+ \cdot \delta s^+ - \delta R^+ \cdot \delta s^- - \delta R^- \cdot \delta s^+ + \delta R^- \cdot \delta s^- \right] \end{array} \right\} \quad (A30)$$

$$\begin{aligned} &+ s \cdot t + \delta s^+ \cdot t - \delta s^- \cdot t + s \cdot \delta t^+ - s \cdot \delta t^- \\ &+ \left[ \delta s^+ \cdot \delta t^+ - \delta s^+ \cdot \delta t^- - \delta s^- \cdot \delta t^+ + \delta s^- \cdot \delta t^- \right] \end{aligned}$$

This final goal function remains quadratic in the delta terms (as is the analytic solution)

and is subject to the following constraints:

$$\begin{aligned} 0 &\leq \delta y^+ \leq \delta y_{\max} \\ 0 &\leq \delta y^- \leq |-\delta y_{\min}| \\ 0 &\leq \delta s^+ \leq \delta s_{\max} \\ 0 &\leq \delta s^- \leq |-\delta s_{\min}| \\ 0 &\leq \delta R^+ \leq \delta R_{\max} \\ 0 &\leq \delta R^- \leq |-\delta R_{\min}| \\ 0 &\leq \delta t^+ \leq \delta t_{\max} \\ 0 &\leq \delta t^- \leq |-\delta t_{\min}| \end{aligned} \quad (A31)$$

The quadratic goal function Eq (A30) can be simplified to the linear goal function from Chapter 2 by assuming  $\delta R$  and  $\delta t$  are negligible compared to  $\delta y$  and  $\delta s$  and setting them equal to zero.



## Appendix B: Final Mathematica Code

A Mathematica notebook for through-fold  
of bounds on exact target loading

### SECTION I.

#### Data Input and Definitions of Functions

*Enter the following data into the Data Input block then evaluate the cell:*

<i>Energy range required:</i>	<i>Erange</i>
<i>number of bins covering eRange:</i>	<i>numBins</i>
<i>number of closed instruments:</i>	<i>nClosed</i>
<i>number of open instruments:</i>	<i>nOpen</i>
<i>fluorescer k-edge of 1st detector:</i>	<i>e0initial</i>
<i>bin spacing (geo or lin):</i>	<i>spacing</i>

```
eRange=64;  
nClosed=8;  
nOpen=4;  
numBins=30;  
spacing=geo;
```

Spectrum Definition:

*Choose a spectrum or create your own. Enter necessary information  
and evaluate cells. Evaluate plot cell to view your selection.*

*Note: only one spectrum can be selected at a time. Evaluate the ClearAll[s ]  
cell prior to defining a second spectrum.*

ClearAll[s]

*Planckian (1 or 2 temp)*

Spectrum Data:

```

kT1=1;
scale1=1;
kT2=1;
scale2=0;

```

Spectrum:

```

s[0]=0;
s[0.0]=0;
s[e_]:=N[scale1(15/(kT1 Pi)^4)(e^3/(Exp[e/kT1]-1)) +
scale2(15/(kT2 Pi)^4)(e^3/(Exp[e/kT2]-1))];

```

```

Plot[s[e_],{e,0,eRange},
  PlotLabel->"Planckian Spectra",
  Frame->True,
  FrameLabel->{"Energy, E/E0", "Amplitude"},
  PlotRange->All];

```

Target Response Definition:

*The same guidance applies as for selection of the spectrum.*

ClearAll[t]

*Broad Gaussian (change shape via mean and standard deviation)*

Gaussian Data:

```

mean=0;
sd=15;
sqrt2pi=N[Sqrt[2Pi]];

```

Gaussian Response:

```

t[e_]:=((1/(sd sqrt2pi)) Exp[(-1/2)((e-mean)/sd)^2]

```

```

PlotLabel->"Gaussian Response Function",
  Frame->True,
  FrameLabel->{"Energy, E/E0", "Amplitude"},
  PlotRange->All];

```

## Detector Systems Definition:

*Evaluate the cells associated with this section. They are based on previous input.*

### K-Edges

```
numInst=nClosed + nOpen;

sqrt2=N[Sqrt[2]];

e0closed=Table[e0initial(sqrt2^n),{n,0,nClosed-1}];

e1closed=Table[2 e0initial(sqrt2^n), {n,0,nClosed-1}];

e0open=Table[e0initial (2^n), {n,0,nOpen-1}];

e0all=Join[e0closed, e0open];
```

### Detector Response Functions

```
rclosed[e0closed_,e1closed_]:=
  Which[e<e0closed,0,
    e0closed<=e<e1closed,
      (1/e)(1-Exp[-2 (e0closed/e)^3])
      (Exp[(-1/4)(e1closed/e)^3]),
    e1closed<=e,
      (1/e)(1-Exp[-2 (e0closed/e)^3])
      (Exp[(-3/2)(e1closed/e)^3])
  ]

ropen[e0open_]:=If[e<e0open,0,
  (1/e)(1-Exp[-3 (e0open/e)^3])
];
```

### Instrument Responses

```
Do[r[i,e_]=rclosed[e0closed[[i]],e1closed[[i]]],
  {i,nClosed}
];

Do[r[i+nClosed,e_]=ropen[e0open[[i]],{i,nOpen}];
```

Energy Bins Definition:

*Evaluate the cells associated with this section. They are base on previous input.*

Bin Spacing:

```
flag=spacing;

deltaEgeo:=Table[N[e0initial(eRange^(i/numBins) -
                  eRange^((i-1)/numBins))
                ],
                {i,1,numBins}
                ];

deltaElin:=N[Table[(eRange-1) e0initial/numBins,
                  {numBins}]];

dE=If[flag==geo, deltaEgeo, flag==lin, deltaElin];
```

Bin Boundaries

```
energyBoundary[0]=e0initial;

eBound=Prepend[Table[energyBoundary[i] = dE[[i]] +
                    energyBoundary[i-1], {i,numBins}],e0initial];

eLower=Drop[eBound,-1];
eUpper=Rest[eBound];
```

Bin Center Energies (for evaluation of functions)

```
eGeoCen=Sqrt[eUpper eLower];
eLinCen=(eUpper + eLower)/2;

eCen=If[flag==geo, eGeoCen, flag==lin, eLinCen];
```

## SECTION II.

### Evaluation of Vectors and Matrices

*Evaluate the cells associated with this section. They are based on previous input.*

Evaluate the Spectrum Vector

```
sVec=Table[s[eCen[[i]]],{i,numBins}];
```

Evaluate the Target Response Vector

```
tCen=Table[t[eCen[[i]]],{i,numBins}];  
tVec=tCen dE
```

Evaluate the Instrument Response Matrix

```
resmatrix=Table[(r[i,#]& /@ eCen) dE,  
                {i,numInst}  
                ];
```

Evaluate the Instrument Signal Vector

```
yCen=resmatrix.sVec
```

Add Random Noise to Signal (Note:  $Y_m=Y+\text{noise}[\ ]$ )

*Noise should NOT be added if using assuming no measurement error.  
If this is the case, define  $y_M=y_{Cen} + 0$  prior to evaluation of the  $y_M$  cell.*

```
<<Statistics`ContinuousDistributions`;  
SeedRandom[1];
```

```
noise[frac_]:=Table[Random[NormalDistribution[0,frac]],  
                   {i,numInst}];
```

```
measErr=noise[.15];
```

```
yM=yCen + (measErr*yCen)
```

## Define All Delta Terms

*The delta terms are set for up to 60 bins, any spacing, and up to 17 detectors.*

*For addiional bins and instruments, the definitions must be extended.*

*The form is self evident.*

*If assuming no measurement error, dYmax and dYmin should be zero vectors.*

```
dSpositive={dSp1,dSp2,dSp3,dSp4,dSp5,dSp6,dSp7,dSp8,  
            dSp9,dSp10,dSp11,dSp12,dSp13,dSp14,dSp15,  
            dSp16,dSp17,dSp18,dSp19,dSp20,dSp21,dSp22,  
            dSp23,dSp24,dSp25,dSp26,dSp27,dSp28,dSp29,  
            dSp30,dSp31,dSp32,dSp33,dSp34,dSp35,dSp36,  
            dSp37,dSp38,dSp39,dSp40,dSp41,dSp42,dSp43,  
            dSp44,dSp45,dSp46,dSp47,dSp48,dSp49,dSp50,  
            dSp51,dSp52,dSp53,dSp54,dSp55,dSp56,dSp57,  
            dSp58,dSp59,dSp60};
```

```
dSnegative={dSn1,dSn2,dSn3,dSn4,dSn5,dSn6,dSn7,dSn8,  
            dSn9,dSn10,dSn11,dSn12,dSn13,dSn14,dSn15,  
            dSn16,dSn17,dSn18,dSn19,dSn20,dSn21,dSn22,  
            dSn23,dSn24,dSn25,dSn26,dSn27,dSn28,dSn29,  
            dSn30,dSn31,dSn32,dSn33,dSn34,dSn35,dSn36,  
            dSn37,dSn38,dSn39,dSn40,dSn41,dSn42,dSn43,  
            dSn44,dSn45,dSn46,dSn47,dSn48,dSn49,dSn50,  
            dSn51,dSn52,dSn53,dSn54,dSn55,dSn56,dSn57,  
            dSn58,dSn59,dSn60};
```

```
dYpositive={dYp1,dYp2,dYp3,dYp4,dYp5,dYp6,dYp7,dYp8,  
            dYp9,dYp10,dYp11,dYp12,dYp13,dYp14,dYp15,  
            dYp16,dYp17};
```

```
dYnegative={dYn1,dYn2,dYn3,dYn4,dYn5,dYn6,dYn7,dYn8,  
            dYn9,dYn10,dYn11,dYn12,dYn13,dYn14,dYn15,  
            dYn16,dYn17};
```

```
dSmax=Table[0.5, {60}];  
dSmin=Table[0.5, {60}];  
dYmax=Table[0.15, {17}];  
dYmin=Table[0.15, {17}];
```

## Write Vectors to Data Files

```
sVec>>spectrum;  
tVec>>target;  
resmatrix>>rMatrix;  
yM>>instSig;
```

```
dYpositive>>dYpos;  
dYnegative>>dYneg;  
dYmax>>dYplus;  
dYmin>>dYminus;
```

```
dSpositive>>dSpos;  
dSnegative>>dSneg;  
dSmax>>dSplus;  
dSmin>>dsminus;
```

\*\*\* Additional Information (*does not need to be evaluated*) \*\*\*

## Exact Instrument Signal

```
Do[y1[i]=NIntegrate[s[e]*r[i,e],  
  {e,e0all[[i]],e1closed[[i]], 64}],  
  {i,nClosed}];  
  
Do[y1[i]=NIntegrate[s[e]*r[i,e],  
  {e,e0all[[i]],64}], {i,nClosed+1,numInst}];  
  
yExact=Table[y1[i],{i,numInst}]
```

## Exact Target Loading

```
zExact=NIntegrate[s[e] t[e], {e, 0, eRange}]
```

## Pseudo-Exact Target Loading

```
pseudoZexact=s.t
```

## SECTION III.

### Definition and Optimization of Exact Target Loading Bounds

- Produces dummy files from datafiles of the required size.
- Defines target loading, maximum, and minimum functions.
- Provides input statements for calculation of:
  - Reads full information from datafiles.
  - Results for no experiment ( $a's=0$ ).
  - FindMinimum[MAXX]
  - FindMinimum[MINN]

Notes: 1) File written to and read from the Mathematica default directory.

2) Numbers in filenames indicate size of file (inst x bins).

3) This file must be run to create the target loading equation and the expressions for use in the maxx and minn commands.

4) The sections starting with "How Many Instruments and Bins in this Test ??" and ending just before "Sample Input Statements for Results" must be evaluated for each combination of instruments that results are desired for.

Remember to change filenames appropriately.

How Many Instruments and Bins to Through-Fold ??

If only desiring the open instruments, enter the TOTAL number of instruments (closed + open) up to the instrument number you are interested in.

```
inst=8;  
bins=30;
```

Read Information From Disk Into Dummy Variables

```
spec=<<spectrum;  
targ=<<target;  
resMat=<<rMatrix;  
signal=<<instSig;
```



```

dYpositive=<<dYpos;
dYnegative=<<dYneg;
dYmax=<<dYplus;
dYmin=<<dYminus;

```

```

dSpositive=<<dSpos;
dSnegative=<<dSneg;
dSmax=<<dSplus;
dSmin=<<dSminus;

```

Read Appropriate Parts of Dummy Variables Into Vectors:

*If only want open instruments and the vectors include both, change the instrument counters from "{i,inst}" to "{i,nclosed+1,inst}" for R, y, dYpos, dYneg, dYplus, and dYminus . It may be easiest to enter the actual number instead of "nclosed+1".*

```

s=Table[spec[[i]], {i,bins}];
t=Table[targ[[i]], {i,bins}];
R=Table[resMat[[i,j]], {i,inst},{j,bins}];
y=Table[signal[[i]], {i,inst}];

```

```

dSpos=Table[dSpositive[[i]], {i,bins}];
dSneg=Table[dSnegative[[i]], {i,bins}];
dSplus=Table[dSmax[[i]], {i,bins}];
dSminus=Table[dSmin[[i]], {i,bins}];

```

```

dYpos=Table[dYpositive[[i]], {i,inst}];
dYneg=Table[dYnegative[[i]], {i,inst}];
dYplus=Table[dYmax[[i]], {i,inst}];
dYminus=Table[dYmin[[i]], {i,inst}];

```

Checking vectors to ensure the right dimensions.

```

Dimensions[y]
Dimensions[R]
Dimensions[s]
Dimensions[t]

```

## Definition of Functions

Target Loading (z):

```
term1=R.s;  
term2=R.(dSpos s);  
term3=R.(dSneg s);  
term4=(dSpos s).t;  
term5=(dSneg s).t;
```

```
z[a_List,dYpos_List,dYneg_List,dSpos_List,  
  dSneg_List]=
```

```
  a.(y + dYpos y - dYneg y - term1 -  
      term2 + term3) +  
  s.t + term4 - term5;
```

Writing target loading function (in Mathematica notation) to a file  
and verifying it is there.

*Note: Only evaluate the second command if you WANT to see a huge eqn.  
or if you are not sure the file was written to disk and want to check.*

**NOMENCLATURE:** *File names indicate target loading (z), validation (val),  
and eight instruments in the equation (8).*

```
%>>z_val8;
```

```
!!z_val8
```

Maximum Target Loading (maxx):

*This is a DIFFERENT correction than for z.*

*If only want open instruments and the vectors include both, change the instrument  
counter from "{i,inst}" to "{i,inst - nclosed}" for dYpos, dYneg, dYplus, and dYminus.  
It may be easiest to enter the actual number instead of "inst - nclosed".*

*Note: There are two counters for dYpos and dYneg each!*

```

maxx[a_List]=

ConstrainedMax[z[a,
  Evaluate[Table[dYpos[[i]],{i,inst}],
    Table[dYneg[[i]],{i,inst}],
    Table[dSpos[[i]],{i,bins}],
    Table[dSneg[[i]],{i,bins}]
  ],

  Evaluate[Flatten[{
    Table[dYpos[[i]]<=dYplus[[i]], {i,inst}],
    Table[dYneg[[i]]<=dYminus[[i]],{i,inst}],
    Table[dSpos[[i]]<=dSplus[[i]], {i,bins}],
    Table[dSneg[[i]]<=dSminus[[i]],{i,bins}]
  }],

  ],

  Evaluate[Flatten[{Table[dYpos[[i]], {i,inst}],
    Table[dYneg[[i]], {i,inst}],
    Table[dSpos[[i]], {i,bins}],
    Table[dSneg[[i]], {i,bins}]
  }],

  ],

];

%>>maval8;

```

Minimum Target Loading (minn):

*This is the SAME correction as for minn.*

*If only want open instruments and the vectors include both, change the instrument counter from "{i,inst}" to "{i,inst - nclosed}" for dYpos, dYneg, dYplus, and dYminus. It may be easiest to enter the actual number instead of "inst - nclosed".*

*Note: There are two counters for dYpos and dYneg each!*

```
minn[a_List]=
```

```

ConstrainedMin[z[a,
  Evaluate[Table[dYpos[[i]],{i,inst}],
    Table[dYneg[[i]],{i,inst}],
    Table[dSpos[[i]],{i,bins}],
    Table[dSneg[[i]],{i,bins}]
  ]
],

Evaluate[Flatten[{
  Table[dYpos[[i]]<=dYplus[[i]], {i,inst}],
  Table[dYneg[[i]]<=dYminus[[i]],{i,inst}],
  Table[dSpos[[i]]<=dSplus[[i]], {i,bins}],
  Table[dSneg[[i]]<=dSminus[[i]],{i,bins}]
  }]
],

Evaluate[Flatten[{Table[dYpos[[i]], {i,inst}],
  Table[dYneg[[i]], {i,inst}],
  Table[dSpos[[i]], {i,bins}],
  Table[dSneg[[i]], {i,bins}]
  }]
]
];

%>>mival8;

```

#### Sample Input Statements for Results

*The form of these input statements will be consistent; however, there are obvious changes based on the number of instruments used and the starting points desired.*

Read datafiles from disk

Target Loading:

```

z[a_List,dYpos_List,dYneg_List,dSpos_List,
  dSneg_List]=<<z_val8;

```

Constrained Maximum:

```

maxx[a_List]=<<maval8;

```

Constrained Minimum:

$\text{minn}[a\_List] = \ll mival8;$

No Experiment,  $a_i$ 's = 0.

$\text{MAXX} = \text{maxx}[\{0,0,0,0,0,0,0,0\}]$

$\text{MINN} = \text{minn}[\{0,0,0,0,0,0,0,0\}]$

Optimizing MAXX and MINN over the Choice of  $a_i$ 's

Minimizing the maximum.

$\text{FindMinimum}[\text{First}[\text{maxx}[\{a_1, a_2, a_3, a_4, a_5, a_6, a_7,$   
 $a_8\}]],$

$\{a_1, -1, 1\}, \{a_2, 1, -1\}, \{a_3, -1, 1\}, \{a_4, 1, -1\},$   
 $\{a_5, -1, 1\}, \{a_6, 1, -1\}, \{a_7, -1, 1\}, \{a_8, 1, -1\}]$

Maximizing the minimum.

*Since we are actually minimizing the negative of the minimum, the result will be the NEGATIVE of the true answer.*

$\text{FindMinimum}[-\text{First}[\text{minn}[\{a_1, a_2, a_3, a_4, a_5, a_6, a_7, a_8\}]],$

$\{a_1, -1, 1\}, \{a_2, 1, -1\}, \{a_3, -1, 1\}, \{a_4, 1, -1\},$   
 $\{a_5, -1, 1\}, \{a_6, 1, -1\}, \{a_7, -1, 1\}, \{a_8, 1, -1\}]$

### Appendix C: Additional Test Results

This appendix is a continuation of the results of Chapter IV. The inputs are the same as defined in Chapter IV.

Table 9. Test Results for Case T1.B

	$a_i$ , Naive Approach	Defined $a_i$	Optimized Max	Optimized Min
a1	0	0	0	0
a2	0	0	0	0
a3	0	0	0	0
a4	0	0	0	0
a5	0	0	0	0
a6	0	0	0	0
a7	0	0	0	0
a8	0	0	0	0
a9	0	1	1	1
a10	0	0	0	0
a11	0	1	1	1
a12	0	0	0	0
$z^U(a)$ , % +	50	18.6	18.6	n/a
$z^U(a)$ , % -	50	12.3	n/a	12.3
Total Bound, %	100	30.9		30.9

Table 10. Test Results for Case T1.C

	$a_i$ , Naive Approach	Defined $a_i$	Optimized Max	Optimized Min
a1	0	1	2.4452	0
a2	0	0	1	0
a3	0	2.5	2.0121	0
a4	0	0	0.1745	0
a5	0	0	3.6246	0
a6	0	0	1.5946	0
a7	0	0	1.3151	0
a8	0	0	-1.9238	0
a9	0	1	0	1.3333
a10	0	0	0	0.923
a11	0	1	0	0.9613
a12	0	0	0	0.035
$Z^U(a)$ , % +	50	15.8	18	n/a
$Z^U(a)$ , % -	50	14.4	n/a	17.1
Total Bound, %	100	30.2		35.1

Table 11. Test Results for Case T2.A

	$a_i$ , Naive Approach	Defined $a_i$	Optimized Max	Optimized Min
a1	0	1	0.769	0.4971
a2	0	0	0.1211	0.9648
a3	0	2.5	3.3036	2.5402
a4	0	0	0	0.9931
a5	0	0	-0.0001	-1.1683
a6	0	0	-0.1288	0.826
a7	0	0	0.0702	-0.6397
a8	0	0	0.0897	0.8914
a9	0	0	0	0
a10	0	0	0	0
a11	0	0	0	0
a12	0	0	0	0
$Z^U(a)$ , % +	50	23.6	18.5	n/a
$Z^U(a)$ , % -	50	26	n/a	17.6
Total Bound, %	100	49.6		36.1



Table 12. Test Results for Case T2.B

	$a_i$ , Naive Approach	Defined $a_i$	Optimized Max	Optimized Min
a1	0	0	2.0801	0
a2	0	0	0.9988	0
a3	0	0	0.6178	0
a4	0	0	0.1997	0
a5	0	0	5.2567	0
a6	0	0	2.0032	0
a7	0	0	1.2941	0
a8	0	0	-2.2269	0
a9	0	1	0	1.1834
a10	0	0	0	-0.03
a11	0	1	0	1.4374
a12	0	0	0	-0.1321
$z^U(a)$ , % +	50	26.7	21.6	n/a
$z^U(a)$ , % -	50	22	n/a	18
Total Bound, %	100	48.7		39.6

Table 13. Test Results for Case T2.C

	$a_i$ , Naive Approach	Defined $a_i$	Optimized Max	Optimized Min
a1	0	1	2.4452	0
a2	0	0	1	0
a3	0	2.5	2.8914	0
a4	0	0	0.612364	0
a5	0	0	4.6113	0
a6	0	0	-0.475	0
a7	0	0	0.001	0
a8	0	0	-0.6234	0
a9	0	1	0	1.3333
a10	0	0	0	1.2265
a11	0	1	0	0.3256
a12	0	0	0	-0.0881
$Z^U(a)$ , % +	50	22.4	15.5	n/a
$Z^U(a)$ , % -	50	21.2	n/a	18.8
Total Bound, %	100	43.6		34.3

Table 14. Test Results for Case T3.A

	$a_i$ , Naive Approach	Defined $a_i$	Optimized Max	Optimized Min
a1	0	1	-0.3123	0
a2	0	0	0.4192	0
a3	0	2.5	1.4946	0
a4	0	0	-0.4488	0
a5	0	0	0.7568	0
a6	0	0	0.459	0
a7	0	0	0.3681	0
a8	0	0	-0.5048	0
a9	0	0	0	0.0993
a10	0	0	0	0.4922
a11	0	0	0	0.0711
a12	0	0	0	0.0218
$Z^U(a)$ , % +	50	55.3	25.6	n/a
$Z^U(a)$ , % -	50	60.9	n/a	19.5
Total Bound, %	100	116.2		45.1

Table 15. Test Results for Case T3.B

	$a_i$ , Naive Approach	Defined $a_i$	Optimized Max	Optimized Min
a1	0	0	0.4492	0
a2	0	0	8.7185	0
a3	0	0	0.4428	0
a4	0	0	-0.1684	0
a5	0	0	2.3099	0
a6	0	0	-0.285	0
a7	0	0	0.4628	0
a8	0	0	-0.4792	0
a9	0	1	0	0.55
a10	0	0	0	0.088
a11	0	1	0	0.5575
a12	0	0	0	0.1326
$Z^U(a)$ , % +	50	55.1	25.9	n/a
$Z^U(a)$ , % -	50	45.5	n/a	23
Total Bound, %	100	100.6		48.9

Table 16. Test Results For Case T3.C

	$a_i$ , Naive Approach	Defined $a_i$	Optimized Max	Optimized Min
a1	0	1	2.4452	0
a2	0	0	1	0
a3	0	2.5	0.2236	0
a4	0	0	-0.076	0
a5	0	0	2.4456	0
a6	0	0	2.5737	0
a7	0	0	2.5825	0
a8	0	0	-3.1688	0
a9	0	1	0	1.191
a10	0	0	0	0.4789
a11	0	1	0	0.4296
a12	0	0	0	0.2164
$Z^U(a)$ , % +	50	36.5	24	n/a
$Z^U(a)$ , % -	50	34.5	n/a	17.7
Total Bound, %	100	71.0		41.7

### Bibliography

- Bevington, Philip R., Data Reduction and Error Analysis for the Physical Sciences. New York: McGraw-Hill Book Company, 1969.
- Burden, Richard L. and Faires, Douglas J., Numerical Analysis. Boston: PWS Publishing Company, 1993.
- Carter, Capt. Michael E., Comparison of Basis Functions and Iteration Solutions to the Fredholm Integral Equation of the First Kind. MS Thesis AFIT/GNE/ENP/89M-1. School of Engineering, Air Force Institute of Technology (AU), Wright-Patterson AFB, OH. March 1989.
- Daniel, Capt. Russell B., An Approximation Technique for Solving a System of Fredholm Integral Equations for Asymmetric detector Response Functions. MS Thesis AFIT/GNE/ENG/88M-3. School of Engineering, Air Force Institute of Technology (AU), Wright-Patterson AFB, OH. March 1988.
- Gorbachencko, G.M., *et al.*, "Use of Fluorescence in the Spectrometry of Pulsed X-Radiation", Instrument and Experimental Technology, 19:244-246 (Jan-Feb 1976).
- Mathews, K.A., Air Force Institute of Technology. Private communications. (1994).
- Miller, 1 Lt. Dennis J., The Feasibility of Cross-Validation as a Parameter Predictor For the Iterative Unfold Method. MS Thesis AFIT/GNE/ENP/90M-5. School of Engineering, Air Force Institute of Technology (AU), Wright-Patterson AFB, OH. March 1990.
- Wing, G.M., A Primer on Integral Equations of the first Kind, The Problem of Deconvolution and Unfolding. Philadelphia: Society for Industrial and Applied Mathematics, 1991.

### Vita

Captain Kris G. Rongone was born 07 December 1963 in Omaha, Nebraska. He graduated from Creighton Preparatory High School in 1982. He attended Iowa State University on an R.O.T.C. scholarship. In 1987 received a Bachelor of Science Degree in Nuclear Engineering. He was commissioned as an Air force officer in May 1987. His first assignment was to the Ballistic Missile Office at Norton AFB, California. At first he worked as a Systems Engineer for the Peacekeeper Rail Garrison Intercontinental Ballistic Missile (ICBM) Program. After a change of program offices, he finished his Norton AFB tour as Lead Project Officer for the Peacekeeper Mk 21 Reentry Vehicle. He entered the Nuclear Engineering program at the Air Force Institute of Technology in June 1993.

Permanent Address: 20 Magnifico Way  
#758  
Hot Springs Village, AR 71909